Applied Energy 375 (2024) 124029

Contents lists available at ScienceDirect

Applied Energy

journal homepage: www.elsevier.com/locate/apenergy

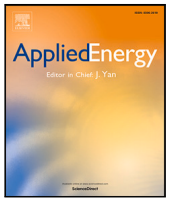

Joint planning of dynamic wireless charging lanes and power delivery infrastructure for heavy-duty drayage trucks

Zuzhao Ye [a], Mikhail A. Bragin [a], Nanpeng Yu [a,*], Ran Wei [b]

[a] Department of Electrical and Computer Engineering, University of California, Riverside, CA, USA
[b] School of Public Policy, University of California, Riverside, CA, USA

ARTICLE INFO

Keywords:
Zero emission
Heavy-duty drayage trucks
Dynamic wireless charging lane
Power delivery infrastructure

ABSTRACT

Heavy-duty drayage trucks pose a considerable emission burden and health risk, primarily due to their operation in densely populated areas around seaports and intermodal terminals. In response to these concerns, governments are setting ambitious targets for zero-emissions drayage truck transition. As such, the widespread adoption of electric drayage trucks is on the horizon. However, one of the main challenges hindering the mass electrification of drayage trucks is the low readiness of charging infrastructure. Traditional charging stations can lead to long waiting times for truck drivers, which can be detrimental to an industry where timely pickup and delivery are crucial. Dynamic wireless charging lanes (DWCLs) have emerged as a promising alternative or supplement to stationary charging stations by enabling charging-on-the-move. Although electric drayage trucks are potentially the most benefited vehicles from DWCLs, the optimal deployment of DWCLs for them is rarely studied. To address this problem, we propose a framework that focuses on the deployment of DWCLs with special attention paid to drayage trucks, while jointly planning the associated power delivery infrastructure. The proposed planning model identifies the optimal locations of DWCLs in a given transportation network and determines how they will be powered by nearby electrical substations. Additionally, the framework also evaluates whether an upgrade of the electrical substation is needed. A large-scale Global Positioning System (GPS) dataset and an electrical substation dataset, which contain more than 7,000 heavy-duty drayage trucks that span over a period of 12 months and over 255 substations, are utilized to provide the necessary input to the proposed framework. We demonstrate the effectiveness of the proposed framework through a case study conducted on a highway network of more than 1,000 miles around the Greater Los Angeles area, home to two of the world's busiest seaports, Port of Los Angeles and Port of Long Beach.

1. Introduction

Reducing greenhouse gas (GHG) emissions from the transportation sector is key to achieving emission reduction targets and mitigating climate change [1]. Although heavy-duty vehicles constitute only 1% of the total vehicle fleet, they account for more than one-quarter of the transportation sector's total GHG emissions [2]. To mitigate their disproportionate contribution to emissions, California has mandated that all medium- and heavy-duty vehicles transition to zero emissions by 2045 [3]. Similarly, in a recently proposed revision to CO_2 standards, the European Union is pushing for a 90% reduction in emissions from trucks by 2040, further underlining the global urgency of decarbonizing heavy-duty vehicles [4].

Drayage trucks are a special type of heavy-duty vehicle that focuses on transporting goods between ports and intermodal terminals [5]. Drayage trucks are usually Class-8 vehicles (the heaviest class) and their prevalent operations in densely populated regions, especially in disadvantaged communities, make them a major source of air pollution and health risks [6]. In response to these issues, regulations in California mandate drayage trucks to achieve full zero-emission status by 2035, a decade ahead of other heavy-duty vehicles [3].

Transportation electrification holds the potential to establish a truly zero-emission ecosystem when coupled with renewable power generation [7]. Therefore, the electrification of drayage trucks would be significantly impactful. However, this ambition is not without challenges. While a segment of drayage trucks traveling less than 200 miles daily may rely solely on overnight home base (depot) charging as per [8], there exists a substantial proportion that undertakes longer journeys. For instance, Kotz et al. [9] reported cases in the New York

* Corresponding author.
E-mail addresses: zye066@ucr.edu (Z. Ye), mbragin@engr.ucr.edu (M.A. Bragin), nyu@ece.ucr.edu (N. Yu), ran.wei@ucr.edu (R. Wei).

https://doi.org/10.1016/j.apenergy.2024.124029
Received 29 July 2023; Received in revised form 3 March 2024; Accepted 23 July 2024

and New Jersey area where drayage trucks covered more than 570 miles in a single day. Meanwhile, Clean Trucks Program [10] found that in Southern California, a large portion of drayage trucks have their maximum per-shift distances greater than 300 miles, with certain trucks covering more than 600 miles. Crucially, as Papson and Ippoliti [11] point out, because the drivers are independent contractors, drayage companies are unable to designate specific trucks as limited-service trucks, such that every truck in the drayage fleet must be a full-service truck, able to complete any run. Therefore, to ensure smooth transitions and uninterrupted business, many fleets will need trucks with high-capacity batteries, which come with high upfront costs and further stimulate the need for high-power charging stations for en-route opportunity charging, potentially resulting in significant grid strain. Moreover, the considerable size of drayage trucks, especially when hauling containers, demands substantial land for charging station siting [12]. This scenario becomes even more complex considering their limited charging opportunities amid pickup or delivery tasks.

Considering the challenges involved in electrifying drayage trucks, charging-in-motion emerges as a promising solution, facilitated by Dynamic Wireless Charging Lanes (DWCLs) [13,14]. The advantages of DWCLs are multifaceted, catering to the diverse interests of various stakeholders. For fleet operators, DWCLs decrease downtime associated with stationary charging, thereby reducing the risk of delivery delays. Policymakers could appreciate the minimal land requirement of DWCLs versus stationary charging stations, a crucial benefit given the scarcity and zoning complications of urban spaces. Meanwhile, electric utility companies can find the DWCLs' charging demand appealing, as it aligns closely with traffic flow, making it more predictable and easier to manage [15,16]. A potential concern for DWCLs is the level of charging power, as drayage trucks require high-power charging. Recent advancements, however, have alleviated this concern. In a recent pilot project, it is reported that Class 8 trucks, given their large undercarriage area, can accommodate up to seven receivers and these receivers can each supply up to 25 kW, enabling a total charging power of 175 kW [17]. Another prototype reported by Askey [18] showcases a further increase in charging power, reaching 120 kW per receiver.

In addition to charging power, the economic feasibility of DWCLs is another concern. Addressing this concern, Chen et al. [19] compared the total costs for a bus transit system using three different charging methods: charging stations, charging lanes, and swapping stations. The findings indicated that while charging lanes incur higher infrastructure costs, the overall cost aligns closely with that of charging stations, benefiting from lower fleet costs due to reduced battery capacity requirements. Beyond bus transit systems, Konstantinou et al. [20] conducted a comprehensive analysis of the economic feasibility of DWCLs along interstate highway I-65 in Indiana for heavy-duty vehicles. The study revealed that the payback period of DWCLs ranges between 20 and 25 years for early adoption deployment. Limb et al. [21] further suggests that the total societal payback period could be shortened to less than 5 years when deployed on primary roads with moderate EV penetration. In a separate study in Auckland, New Zealand, Majhi et al. [22] highlighted an additional benefit of DWCLs: as the charging power of DWCLs increases, the time savings from reduced trips to static charging stations become substantial. A significant but often overlooked external cost of DWCLs is the congestion cost incurred during the construction phase. This is a challenge that is not faced by other charging methods. Therefore, it would be highly beneficial to align the deployment of DWCLs with road pavement replacement or maintenance [20]. Such a strategy will minimize both congestion events and civil engineering demands, reducing them to a single occurrence rather than multiple disruptions.

DWCLs have gained traction globally with several demonstration projects underway, including a recent one-mile pilot project initiated in Detroit, Michigan marking the first such program on a U.S. public road [23]. Prior to this, various European demonstration projects had already been deployed, including a 0.7-mile (1.05 km) intercity toll road in Italy and a 1-mile (1.65 km) public road in Sweden [24], Particularly, Sweden's policymakers aim to have 1,243 miles (2,000 km) of electrified roadway in operation by 2030 [17], with inductive wireless charging being one of the three candidate charging methods [25]. Given these undertakings, the broader implementation of DWCLs seems on the horizon. The deployment of DWCLs for drayage trucks holds special significance for California, a state with multiple large seaports and intermodal terminals. Combined with stationary plug-in charging stations, DWCLs will lower the barrier to electrifying drayage trucks. The gradual replacement of fossil-fueled trucks with electric ones is anticipated to reduce air pollutants significantly. This change is especially meaningful for disadvantaged communities in California that are often disproportionately affected by air pollution due to their proximity to ports and intermodal terminals [26]. Furthermore, in places like California where there is excess daytime solar generation, DWCLs can help reduce solar curtailment by allowing electric drayage trucks to function as "moving batteries" during their operations, thereby saving the costs needed for stationary energy storage.

Despite the prospects, some key questions must be answered before the widespread deployment of DWCL can begin. Firstly, it is essential to identify the optimal deployment locations for these lanes to best serve the drayage trucks. This involves understanding which routes the trucks are traveling frequently and how much time they spend on these routes. Secondly, the power source for the DWCLs needs to be addressed. This includes determining the routes of electric power lines between electrical substations and DWCLs and the power flow on these lines. Thirdly, the existing substations need to be upgraded to accommodate the increased demand from DWCLs. This involves deciding whether to increase the load hosting capacity of existing substations and if so by how much. Last but not least, although it falls outside the scope of this study, the overall cost of DWCLs versus alternative charging methods (e.g. plug-in charging and battery swapping) should be evaluated on a case-by-case basis. These problems should be addressed holistically to ensure that the system is designed in the most cost-effective way and to facilitate cross-agency collaboration during development.

In this research, we propose to deploy the DWCLs for drayage trucks that serve the Greater Los Angeles area, consisting of the Port of Long Beach and the Port of Los Angeles, two of the largest seaports in the world. We will utilize large-scale real-world GPS data from over 7,000 drayage trucks with a time span of over a year and real-world data on electrical substations from a major regional electric utility company. A comprehensive optimization model will be established to determine where to deploy DWCLs on a highway network of more than 1,000 miles. The optimization model will also identify the power source of DWCLs from nearby electrical substations and whether to take advantage of the remaining load hosting capacity of the electrical substations or to upgrade them.

This article is outlined as follows: Section 2 provides a comprehensive review of the literature. Section 3 highlights the contributions of this article. Section 4 formulates the overall optimization framework, including the objectives and the necessary constraints and assumptions. Section 5 introduces the selected study area and how the required input data are obtained and processed. Section 6 summarizes the solution method to address the computational complexity associated with solving the optimization problem. Section 7 presents the optimization results and analyzes their impacts and implications. Finally, conclusions and suggestions for future research are presented in Section 8.

2. Literature review

Current research on DWCL planning spans a wide range of aspects. These studies can be organized based on either the vehicle types or the power supply systems under consideration in cases where joint DWCL and power system planning are involved.

2.1. Categorized by vehicle types

Much work is devoted to transit buses that are running on fixed routes. Early pioneering work in this regard was carried out by Jeong et al. [27] where the goal is to deploy a set of power tracks (i.e. DWCL segments) along a circled route to reduce the required battery size of buses. Liu and Song [28] again focused on DWCLs for fixed-route electric buses, however, a more complex bus system with multiple bus lines is considered altogether instead of a single route. Alwesabi et al. [29] further extend the framework to jointly schedule the electric buses and Helber et al. [30] employed a similar methodology to support the deployment of DWCLs for electric airport passenger buses.

Besides transit buses, the majority of the other work focuses on general traffic instead. In Riemann et al. [31], DWCL deployment is optimized to capture maximum traffic flow under stochastic user equilibrium. Chen et al. [32] developed a model to assess user preferences and public benefits of DWCLs compared to stationary charging, determining optimal DWCL length along a straight corridor. In addition to optimizing locations, Bi et al. [33] considers the remaining service life of pavement to optimize the timing of deployment. Traffic signals can cause stop-and-go traffic and impact DWCLs' energy supply. Li et al. [34] addressed this issue using a cell transmission model, assuming varying charging powers for stationary and dynamic charging. Xia et al. [35] applied traffic wave theory instead and correlated energy supply with traffic density dynamics. DWCLs can alter drivers' behavior and adversely impact traffic. For instance, EVs might drive slower on DWCLs to absorb more power, leading to slower traffic and increasing the possibility of overtaking maneuvers, which further reduces the road capacity, as modeled by He et al. [36]. On the other hand, if the benefits outweigh the costs, drivers may still prefer DWCLs despite longer travel time. This phenomenon is addressed by sequential two-level planning models that are developed under either user equilibrium [37,38] or system optimum principles [39]. Ushijima-Mwesigwa et al. [40] considered another aspect of DWCL planning which is minimizing the number of ‘‘infeasible routes’’—those causing a significant SoC drop, thereby aiming to bolster driver confidence. Konstantinou et al. [20] adopted a multifaceted approach by taking into account factors like demand, cost, EV-specific, and environmental criteria (e.g., floodplains) to calculate suitability indices of DWCLs for each highway segment.

2.2. Categorized by power systems involved

The power supply for DWCLs typically involves two stages: (1) Grid connection where power is sourced from local electrical substations and converted by step-down transformers, and (2) Local conversion, where the AC power from the grid is converted to high-frequency power for the wireless charging system through a set of rectifier-inverter structures [41,42].

Research focused on fixed-route transit applications usually pays less attention to the grid connection and instead emphasizes on optimizing local conversions. In this context, Liu and Song [28] introduced a model that treats a complete DWCL facility as a node (inverter) connected to a series of links (charging pads). As an inverter comes with a fixed cost, the model implicitly minimizes investment costs by connecting as many pads to one inverter as possible. Despite its wide use, such as by Helber et al. [30] and Alwesabi et al. [29], this method's notable drawback is the ignored power capacity limit, given the presumption that an unlimited number of charging pads can link to a single inverter [30].

Only a few studies explicitly take into account grid connection. Xia et al. [35] addressed this issue by considering the construction of new cables along existing lines to maintain power balance and nodal voltage levels. However, the interconnections between DWCLs and substation upgrades were mostly overlooked. Konstantinou et al. [20] addressed these overlooked factors in a rule-based approach, assuming substations will first power the nearest DWCL segments, with expanding coverage based on available load hosting capacity. When several substations can power the same segments, the substation with the highest power-to-cable distance ratio is selected. While this rule-based approach works for simple scenarios with limited DWCL segments and substations, it becomes inefficient and does not guarantee optimality for larger, more complex networks.

3. Contribution

Upon a careful review of existing literature, we outline the key contributions of this study as follows:

- Firstly, while previous studies have mainly concentrated on the deployment of DWCLs for electric buses or general traffic, there is an absence of research specifically targeting drayage trucks, which contribute significantly to urban pollution but require increased infrastructure support before electrification. Such gap is addressed in this research.
- Secondly, we explore a holistic approach to answer the interconnected questions regarding DWCL deployment, grid connections, and power system upgrades. Most previous studies primarily concentrated on optimizing DWCL placement only, with limited attention paid to the power supply of DWCLs or the capacity of the power system behind them.
- Last but not least, this study covers a large regional highway network exceeding 1,000 miles and leverages large-scale GPS data for realistic inputs to the framework, delivering practical insights to policymakers and demonstrating a methodology pipeline that can be replicated in other regions.

This research is expected to offer strategic support for cross-agency collaborations in the development of DWCLs, ultimately facilitating the smooth transition towards a zero-emission drayage industry.

4. Model formulation

4.1. Problem description

The primary focus of this research is to integrate DWCLs into a regional highway network, serving as an essential part of the electric power ecosystem for electric drayage trucks, as depicted in Fig. 1. To source power, DWCLs need to be connected with nearby electrical substations via a series of lines traversing land or roads, and paired with step-down transformers. On the other hand, the electricity demand on DWCLs is also related to the traffic of electric drayage trucks. Therefore, to support the optimal deployment of DWCLs, we will jointly consider the upstream power distribution system that supplies electricity to DWCLs, as well as the downstream demand from electric drayage trucks.

Specifically, the highway network will be divided into a set of I segments, with each segment evaluated individually for potential wireless charging system installation and connection with the grid. The division of the highway into segments and the gathering of traffic data for each segment will be conducted via specific procedures and algorithms, based on a GPS dataset. More details on these procedures will be provided in Section 5.2. We adopt the assumptions in Konstantinou et al. [20] that the wireless charging system will be installed on the right lane of a multi-lane highway. As a truck enters the designated lane, transmitter coils embedded beneath the pavement will transmit power to receivers mounted on the truck's undercarriage via magnetic resonance induction [17,41].

The objective of the optimization framework will be maximizing the annual electricity supplied to drayage trucks by DWCLs, while considering constraints of DWCL contiguity, grid connection, electrical substation hosting capacity, line losses, and budget threshold. The objectives and constraints will be introduced in detail in this section. The decisions include where DWCLs are deployed, how the DWCLs are connected to the electrical substations, and whether upgrades of the electrical substations are necessary. The key notations used in this study are consolidated in Table 1.

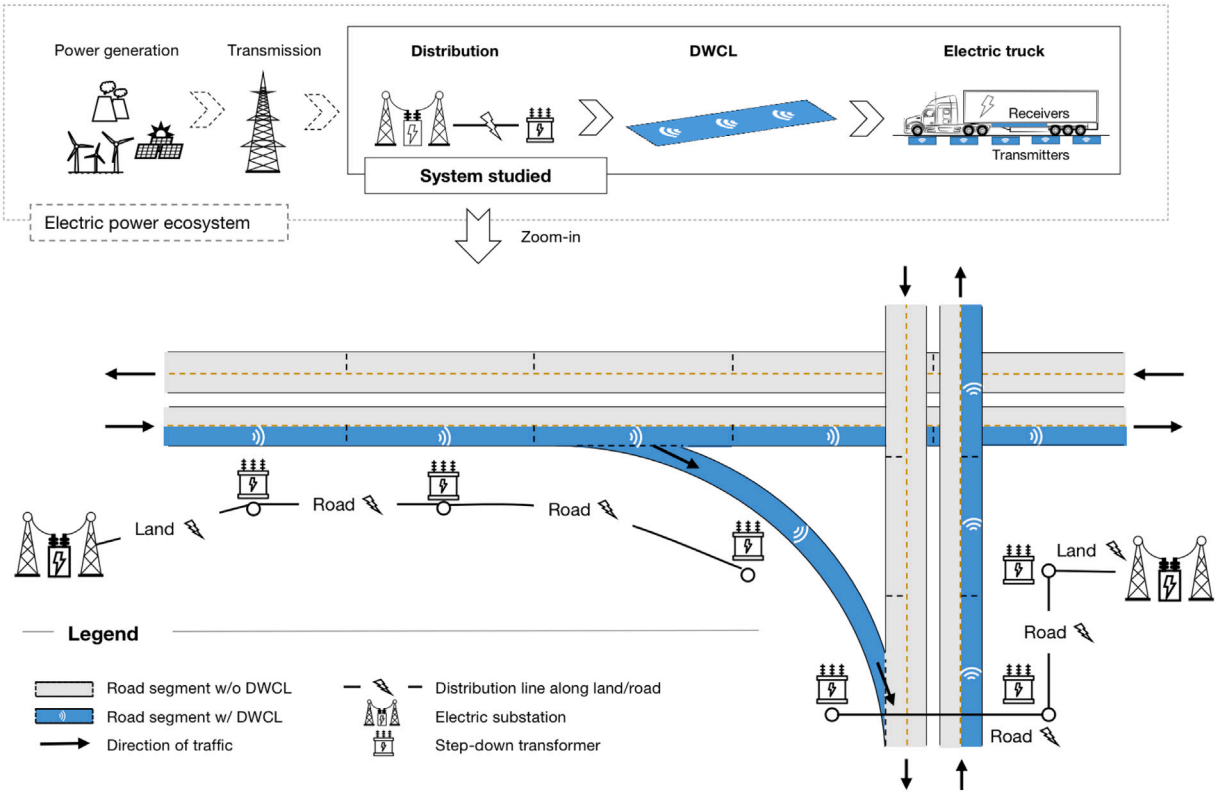

Fig. 1. An illustration of the systems studied.

4.2. Objective function

First of all, the objective of the optimization framework is to maximize E^{tot}, the total annual electricity supplied to trucks by all DWCL segments:

$$\max \quad E^{tot} \tag{1}$$

For a segment i with DWCL, the amount of electricity it can supply to trucks is determined by the aggregated charging power and the dwell time of trucks. For practical consideration, the aggregated charging power will have an upper limit which is the power capacity of a DWCL segment. If the number of trucks is less than a threshold $\overline{n}_i$, the aggregated charging power will grow linearly with the number of trucks - a phase referred to as normal charging, where each truck can charge at its rated power p^{truck}. We assume the receiving areas under the trucks are uniform and $p^{truck} = 175$kW [17]. If the number of trucks surpasses the threshold, the actual charging power will be maintained at the DWCL segment's power capacity - a phase referred to as saturated charging. Under the assumption that the receiving areas under the trucks are uniform, the total power in this phase will be distributed evenly among all the trucks. Fig. 2 illustrates this concept with a segment that has a power capacity of 1 MW and the consequent threshold truck number $\overline{n}_i = 5$. With this understanding, the total annual energy supplied E^{tot} can be defined as:

$$E^{tot} = \sum_{i \in I} \left[\underbrace{\sum_{n=0}^{\overline{n}_i} p^{truck} \cdot n \cdot t_i(n)}_{\text{Normal Charging}} + \underbrace{\sum_{n=\overline{n}_i+1}^{\infty} \rho \cdot l_i \cdot t_i(n)}_{\text{Saturated Charging}} \right] x_i, \tag{2}$$

$$\overline{n}_i = \left\lfloor \frac{\rho \cdot l_i}{p^{truck}} \right\rfloor, \forall i \in I, \tag{3}$$

where $\overline{n}_i = \left\lfloor \frac{\rho \cdot l_i}{p^{truck}} \right\rfloor$ denotes the threshold number of trucks for segment i, ρ is the power capacity per unit length of DWCL, and l_i is the length of segment i. The term $t_i(n)$ denotes the duration when exactly n trucks are present on segment i within a specified period (one year in this study). x_i is a binary decision variable indicating whether highway segment i is converted into a DWCL segment, with $x_i = 1$ suggesting the segment has been converted.

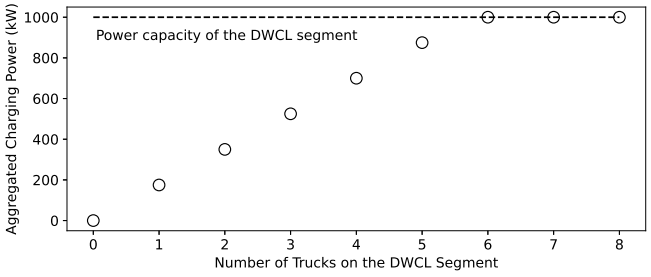

Fig. 2. An illustration of the power capacity limit of a road segment.

4.3. System constraints

4.3.1. Contiguity

In consideration of the economy of scale and to ensure a sufficient energy supply as trucks traverse the DWCLs – a critical aspect for fleet scheduling – we require that the continuous stretch of DWCL along the direction of traffic should not be less than a specific length threshold, L_{thres}. To implement this requirement, we introduce a concept of a minimum set of contiguous segments along the traffic direction, which we abbreviate as a "set of contiguous segments" or an "SCS" for simplicity. SCSs are formed by connecting adjacent segments until their combined length reaches the length threshold L_{thres}. Fig. 3 illustrates this concept with three examples of SCS using hatch patterns, assuming the threshold length is three units and each segment has a length of one unit. It is important to note that when constructing an SCS, ramps are

Table 1
Summary of notations for sets, parameters, and decision variables.

	Sets
I	The set of index of all road segments.
J	The set of index of all SCSs.
K	The set of index of all electrical substations.
I_j	The subset of I that consists of all segments belonging to the jth SCS.
J_i	The subset of J that consists of all SCSs in which road segment i is a member.
K_i	The subset of K that consists of all nearby electrical substations that segment i can connect with.
N_i	The subset of I that consists of all nearby segments that segment i can connect with.
	Parameters
l_i	Length of road segment i.
T	Study time period (one year).
ρ	Power capacity of a unit length of DWCL (default value 2 MW/mile).
$t_i(n)$	Total truck dwell time on segment i within the study period when there are n trucks present on segment i.
$\overline{n}_i$	Maximum number of trucks segment i can support charging at the rated charging power.
p^{truck}	Rated charging power of a truck (175 kW).
L_{thres}	Minimal threshold length of a contiguous stretch of DWCL segments (10 miles).
d_{ki}	Distance between substation k and segment i.
$d_{i'i}$	Distance between segments i' and i.
r_{ki}	Line resistance between substation k and segment i.
$r_{i'i}$	Line resistance between segments i' and i.
$P_k^{rmc,ini}$	Initial remaining load hosting capacity of substation k
$P^{up,std}$	Standard amount of capacity upgrade of substations
LF	Typical load factor (0.5).
PF	Typical power factor (0.95).
U^{line}	Typical line-line voltage of the power distribution line (13.8 kV).
c^{dwcl}	Unit cost of DWCL, including annual maintenance ($664,642/mile, amortized).
c^{trns}	Unit cost of step-down transformers ($22,034/MW, amortized).
c^{line}	Unit cost of power distribution lines ($127,295/mile, amortized).
c^{loss}	Unit cost of line losses ($100/MWh).
$c^{up,fix}$	Fixed cost of substation upgrade ($506,773/upgrade, amortized).
$c^{up,var}$	Variable cost of substation upgrade ($22,034/MW, amortized).
B	Annual budget.
	Decision Variables
x_i	$x_i = 1$ indicates installation of DWCL on road segment i. Otherwise, $x_i = 0$.
y_j	$y_j = 1$ indicates installation of DWCL on SCS j. Otherwise, $y_j = 0$.
p_i	The power demand of segment i.
$p_{i'i}^{road}$	The power supply from segment i' to i.
$\widehat{p_{i'i}^{road}}$	A binary variable indicating if there is a line between segments i' and i.
p_{ki}^{land}	The power supply from substation k to segment i.
$\widehat{p_{ki}^{land}}$	A binary variable indicating if there is a line between substation k and segment i.
$I_{i'i}^{road}$	The current flow on the line between segments i' and i.
I_{ki}^{land}	The current flow on the line between substation k and segment i.
$L_{i'i}^{road}$	Electricity loss on the line between segments i' and i.
L_{ki}^{land}	Electricity loss on the line between substation k and segment i.
P_k^{up}	Total capacity upgrade at substation k.
$P_k^{up,var}$	Variable part of capacity upgrade at substation k.
$\widehat{P_k^{up}}$	A binary variable indicating if there is an upgrade at substation k.

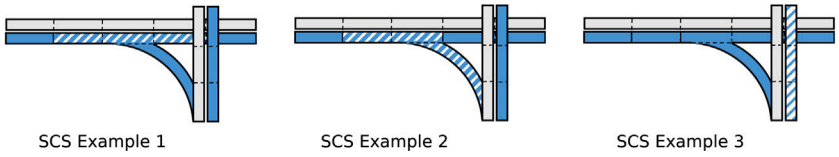

Fig. 3. Examples of SCSs.

also taken into account in conjunction with main roadways. We have initially set L_{thres} to 10 miles and its value can be adjusted based on varying regional needs and conditions. With the understanding of SCS, we can derive a set J that contains all potential SCSs. This is practically achieved through a recursive algorithm, the details of which can be found in Appendix A for interested readers.

We use I_j and J_i to denote the mapping relationships between individual segments to SCSs. I_j is a subset of I that consists of all road segments in SCS j. Correspondingly, J_i is a subset of J that consists of all SCSs in which road segment i is a member. A binary variable y_j denotes whether an SCS j is entirely installed with DWCL and $y_j = 1$ implies each segment within SCS j is a DWCL segment. We then define constraints (4) and (5) to ensure the minimum contiguous length condition is satisfied.

First, to qualify a segment i as a DWCL segment ($x_i = 1$), it must belong to at least one SCS where all segments are DWCL segments, that is, $\sum_{j\in J_i} y_j \geq 1$. Conversely, if none of the SCSs in J_i meet the minimum contiguous length condition, i.e. $y_j = 0, \forall j \in J_i$, segment i is not qualified as a DWCL segment ($x_i = 0$). Constraint (4) encapsulates these two cases:

$$\sum_{j\in J_i} y_j \geq x_i, \quad \forall i \in I. \tag{4}$$

Second, if SCS j is fully equipped with DWCL ($y_j = 1$), it naturally follows that all segments within SCS j are DWCL segments, i.e. $x_i = 1, \forall i \in I_j$. However, if $y_j = 0$, a road segment within SCS j could either be a DWCL segment or not, since this road segment could be a member of other SCSs. Constraint (5) represents these two scenarios:

$$x_i \geq y_j, \quad \forall j \in J, \forall i \in I_j. \tag{5}$$

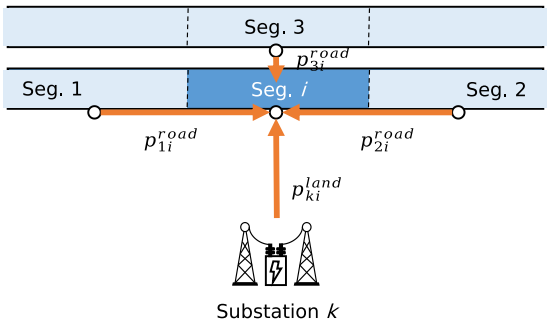

Fig. 4. An illustration of the power balance of Segment i through connections with nearby segments and substations.

The combination of constraints (4) and (5) ensures that no DWCL segments can be built outside of a fully electrified SCS, which naturally fulfills the minimum contiguous length condition.

4.4. Grid connection

DWCLs as a whole system will be powered through connections with the electrical substations. At a lower-level scheme, a specific individual DWCL segment can obtain power from nearby electrical substations and/or through connections with nearby DWCL segments, which have established connections with the grid. For example, as shown in Fig. 4, the power demand for segment i is satisfied by supplies from nearby substation k and nearby segments 1, 2, and 3. We encapsulate this relationship in (6):

$$p_i = \sum_{i' \in N_i} p_{i'i}^{road} + \sum_{k \in K_i} p_{ki}^{land}, \quad \forall i \in I, \tag{6}$$

$$p_i = \rho \cdot l_i \cdot x_i, \quad \forall i \in I, \tag{7}$$

where p_i is the power demand of segment i and it is determined by the unit-length power capacity of DWCL (ρ), the segment length (l_i), and x_i. Power supplied from nearby segment i' to segment i will be transferred through a distribution line along the road, and it is denoted as $p_{i'i}^{road}$, while p_{ki}^{land} represents power supplied from a nearby substation k to segment i via a land-based distribution line. The set of nearby segments to segment i is defined as N_i, which includes its adjacent segments and the three nearest segments besides the adjacent ones. Similarly, the five nearest substations to segment i are considered in set K_i. This setup means that segment i can connect with multiple segments and substations simultaneously, with the optimization model determining the best configuration.

The power supplies between road segments are mutual: If segment i' is supplying power to segment i, equivalently segment i is also drawing power from segment i', resulting in a power deficit in segment i', as indicated in (8). Such a deficit must eventually be compensated by the power supply from nearby segments of i' and/or its nearby substations.

$$p_{ii'}^{road} = -p_{i'i}^{road}, \quad \forall i \in I, \forall i' \in N_i. \tag{8}$$

On the other hand, the power supply from substations will always be non-negative:

$$p_{ki}^{land} \geq 0, \quad \forall i \in I, \forall k \in K. \tag{9}$$

A connection between two segments is only possible when both are DWCL segments, as stated in (10). Likewise, a connection between a segment and a substation also requires the segment to be a DWCL segment, as per (11).

$$\widehat{p_{i'i}^{road}} \leq min(x_i, x_{i'}), \quad \forall i \in I, \forall i' \in N_i, \tag{10}$$

$$\widehat{p_{ki}^{land}} \leq x_i, \quad \forall i \in I, \forall k \in K. \tag{11}$$

$\widehat{p_{i'i}^{road}}$ and $\widehat{p_{ki}^{land}}$ are two types of binary variables introduced to denote the presence of connections, as detailed in (12) and (13). These variables will also help us formulate the cost of constructing distribution lines in Section 4.7.

$$\widehat{p_{i'i}^{road}} = \begin{cases} 1, & \text{if } p_{i'i}^{road} \neq 0 \\ 0, & \text{otherwise,} \end{cases} \tag{12}$$

$$\widehat{p_{ki}^{land}} = \begin{cases} 1, & \text{if } p_{ki}^{land} > 0 \\ 0, & \text{otherwise.} \end{cases} \tag{13}$$

4.5. Electrical substation upgrade

An electrical substation has a certain power supply limit, also referred to as the load hosting capacity (or load integration capacity) [43]. The remaining load hosting capacity of a substation k, denoted as P_k^{rmc}, is the difference between the load hosting capacity and the current peak load. The remaining load hosting capacity should be sufficient to support the loads from all DWCL segments it is connected to, as shown in (14).

$$P_k^{rmc} \geq \sum_{i \in I} p_{ki}^{land}, \quad \forall k \in K \tag{14}$$

An upgrade will potentially be triggered to increase the remaining load hosting capacity:

$$P_k^{rmc} = P_k^{rmc,ini} + P_k^{up}, \quad \forall k \in K, \tag{15}$$

where $P_k^{rmc,ini}$ is the initial remaining load hosting capacity of substation k, and P_k^{up} denotes the capacity increase after an upgrade. Typically, the literature presents two main approaches to substation upgrades. One method assumes a fixed upgrade without a variable component [44,45]. The other employs a stepwise upgrade method, where the capacity is increased in incremental steps [46,47]. Considering that the fixed costs, including planning & permitting, site work, protection & control, and overhead services, are significant in the study area, while the equipment cost is comparatively less, we have chosen to apply a method that combines a major fixed upgrade cost with a variable component:

$$P_k^{up} = P^{up,std} \cdot PF \cdot \widehat{P_k^{up}} + P_k^{up,var}, \quad \forall k \in K \tag{16}$$

Once an upgrade is needed, a standard transformer with a specific MVA rating of $P^{up,std}$ will be selected, indicating the minimal fixed capacity upgrade. PF is the typical power factor and $\widehat{P_k^{up}}$ is a binary variable signaling if an upgrade is triggered. A value of 1 for $\widehat{P_k^{up}}$ indicates an upgrade is triggered. Also, note that the variable component of an upgrade, $P_k^{up,var}$, is only applicable when $\widehat{P_k^{up}} = 1$, as stated in (18), where M is a relatively large number.

$$\widehat{P_k^{up}} \in \{0, 1\}, \quad \forall k \in K, \tag{17}$$

$$0 \leq P_k^{up,var} \leq M \cdot \widehat{P_k^{up}}, \quad \forall k \in K. \tag{18}$$

In practice, the total upgrade, which includes both the fixed and variable components, will be aligned with the closest power ratings of transformers available on the market. Importantly, this aligned transformer power rating should be higher than the calculated total to ensure adequacy and reliability. Other components necessary for upgrades, e.g. circuit breakers and capacitor banks, will be selected to complement this alignment.

4.6. Distribution line losses

Line losses due to Joule heating (or resistive heating) can be costly in power system operations. In a three-phase distribution system, the line losses for road and land distribution lines can be formulated as per (19) and (20):

$$L_{i'i}^{road} = 3 \cdot \left(I_{i'i}^{road}\right)^2 \cdot r_{i'i} \cdot T, \quad \forall i' \in N_i, \forall i \in I, \tag{19}$$

$$L_{ki}^{land} = 3 \cdot \left(I_{ki}^{land}\right)^2 \cdot r_{ki} \cdot T, \quad \forall i \in I, \forall k \in K, \tag{20}$$

where $I_{i'i}^{road}$ and I_{ki}^{land} are the line currents; $r_{i'i}$ and r_{ki} denote the line resistance; T is the study time period. The line currents are derived from the following relationships that connect power, voltage, and current:

$$p_{i'i}^{road} \cdot LF = \sqrt{3} \cdot U^{line} \cdot I_{i'i}^{road} \cdot PF, \quad \forall i' \in N_i, \forall i \in I, \tag{21}$$

$$p_{ki}^{land} \cdot LF = \sqrt{3} \cdot U^{line} \cdot I_{ki}^{land} \cdot PF, \quad \forall i \in I, \forall k \in K, \tag{22}$$

where LF is the typical load factor and U^{line} is the line-to-line voltage of the distribution system. The line current is also subject to the limitations of the conductor and it should not exceed a certain maximum value:

$$I_{i'i}^{road}, I_{ki}^{land} \leq I^{max}. \tag{23}$$

4.7. Budget

The development of the DWCLs will operate within an annual budget of B. The costs of hardware, including DWCL deployment, transformer pairing, distribution line installation, and substation upgrade, will be amortized and converted into annual costs. The overall cost of development is divided into four components:

- The deployment cost of DWCL segments is presumed to be proportional to the length of DWCL segments, with c^{dwcl} (in \$/mile) as the unit cost, covering not only the civil projects and the charging system, but also the annual maintenance. Additionally, we factor in the congestion cost, an external societal cost incurred during the construction of DWCLs, as part of c^{dwcl} in a comparative analysis detailed in Section 7.4. Moreover, transformers are necessary to step down the medium-level line-to-line voltage U^{line} (e.g., 13.8 kV) to low levels (e.g., 480 V) suitable for DWCLs [41]. The cost of transformers is assumed to be proportional to the power demand, which, in turn, is proportional to the length of DWCLs. The unit cost of a transformer is c^{trns} (in \$/MW).
- The installation of distribution lines along roads and land. We consider the cost of a distribution line to be proportional to the length of the line, and c^{line} (in \$/mile) is the unit cost. As the right-of-way along public roadways is well established, road installations are less costly compared to land installations [48], which require land acquisition. Therefore, we introduce a discount factor λ to account for the reduced cost of installations along roads. In addition, since the connections between segments are mutual, we multiply the cost of road installation by 1/2 to avoid double-counting. The distance between two segments, $d_{i'i}$, is estimated between their midpoints, while the distance between a segment and a substation, d_{ki}, is calculated based on their shortest distance.
- The upgrade of substations. The cost associated with upgrading substations has two components. A fixed cost $c^{up,fix}$ is incurred once an upgrade is triggered. If additional load hosting capacity is required beyond the standard upgrade, the supplementary cost is proportional to the variable capacity upgrade amount, with $c^{up,var}$ (in \$/MW) as the unit cost.
- Line losses. The cost of line losses is denoted by c^{loss} (in \$/MWh). Similar to the installation of road distribution lines, line losses on road distribution lines are halved to prevent double counting.

$$\underbrace{\left(c^{dwcl} + \rho \cdot c^{trns}\right) \sum_{i \in I} l_i \cdot x_i}_{\text{DWCL deployment and pairing transformers}} + \underbrace{c^{line} \sum_{i \in I} \left(\lambda \cdot \frac{1}{2} \cdot \sum_{i \in N_i} d_{i'i} \cdot \widehat{p_{i'i}^{road}} + \sum_{k \in K} d_{ki} \cdot \widehat{p_{ki}^{land}} \right)}_{\text{Distribution lines installation along roads and land}} + \tag{24}$$

$$\underbrace{\sum_{k \in K} \left(c^{up,fix} \cdot \widehat{P_k^{up}} + c^{up,var} \cdot P_k^{up,var} \right)}_{\text{Substation upgrade}} + \underbrace{c^{loss} \sum_{i \in I} \left(\frac{1}{2} \cdot \sum_{i \in N_i} L_{i'i}^{road} + \sum_{k \in K} L_{ki}^{land} \right)}_{\text{Lines losses}} \leq B.$$

4.8. Summary of the model

The joint DWCL and power system planning model will target the objective function as outlined in (1) and comply with constraints (2)–(24). In particular, (12) and (13) will be linearized using standard techniques (refer to Appendix B for more details). The resultant optimization problem is a Mixed Integer Quadratically Constrained Program (MIQCP), which can be effectively solved using commercial solvers under a tailored solution method. We will introduce the details of the solution method in Section 6.

5. Data description

In this section, we get into the details regarding key data sources and data processing methods used in our study. We begin with introducing our study area and road network, followed by how we derive road segments and dwell time statistics from GPS data of drayage trucks. We then explain the details of the electrical substations information used in this study. Cost estimations are also provided for various aspects of DWCLs and the power system.

5.1. Study area and road network

Our study is concentrated on the highway network within the Greater Los Angeles area, which is home to two of the world's busiest seaports, the Port of Long Beach and the Port of Los Angeles. The annual traffic density of trucks along preselected major highways is depicted in Fig. 5(a). Zooming in on the port area, as illustrated in Fig. 5(b), there are several major interstate highways and state routes running through, such as I-710, I-110, SR-91, and so forth. In addition to the main sections of highways, we also account for intersections and ramps, as seen in Fig. 5(c), which provides a closer view. The total highway length under consideration in this study is 1,052 miles. The traffic density is calculated from trucks' GPS trajectory data, with further details to be explained in Section 5.2.

5.2. GPS drayage truck trajectory data

The set of road segments I and truck dwell time statistics $t_i(n), \forall i \in I$ are derived from a GPS trajectory dataset, which comprises 7,150 drayage trucks over a 12-month period from July 2021 to June 2022. About 33,500 drayage trucks annually service California's seaports and railyards [6], implying that the GPS dataset used in this study represents roughly 20% of the total drayage trucks.

5.2.1. From GPS data to road segments

Our first goal is to obtain the set of road segments I, which requires dividing the road network into segments of a length of approximately 1 mile. While a manual division of the road network is an option, it will be tedious for large networks, especially when taking complex intersection ramps into account. Therefore, we utilize GPS data to automatically segment the roads. This process is achieved through a combination of specifically designed algorithms. In the first step, we calculate the shortest path between each pair of GPS data points using ESRI StreetMap Premium and ArcPro network analyst [49] to transform the raw GPS data points into trajectories along existing roadways. These trajectories, comprising a list of points on the roadways, are then segmented by linking the leading and trailing points in sequence, and

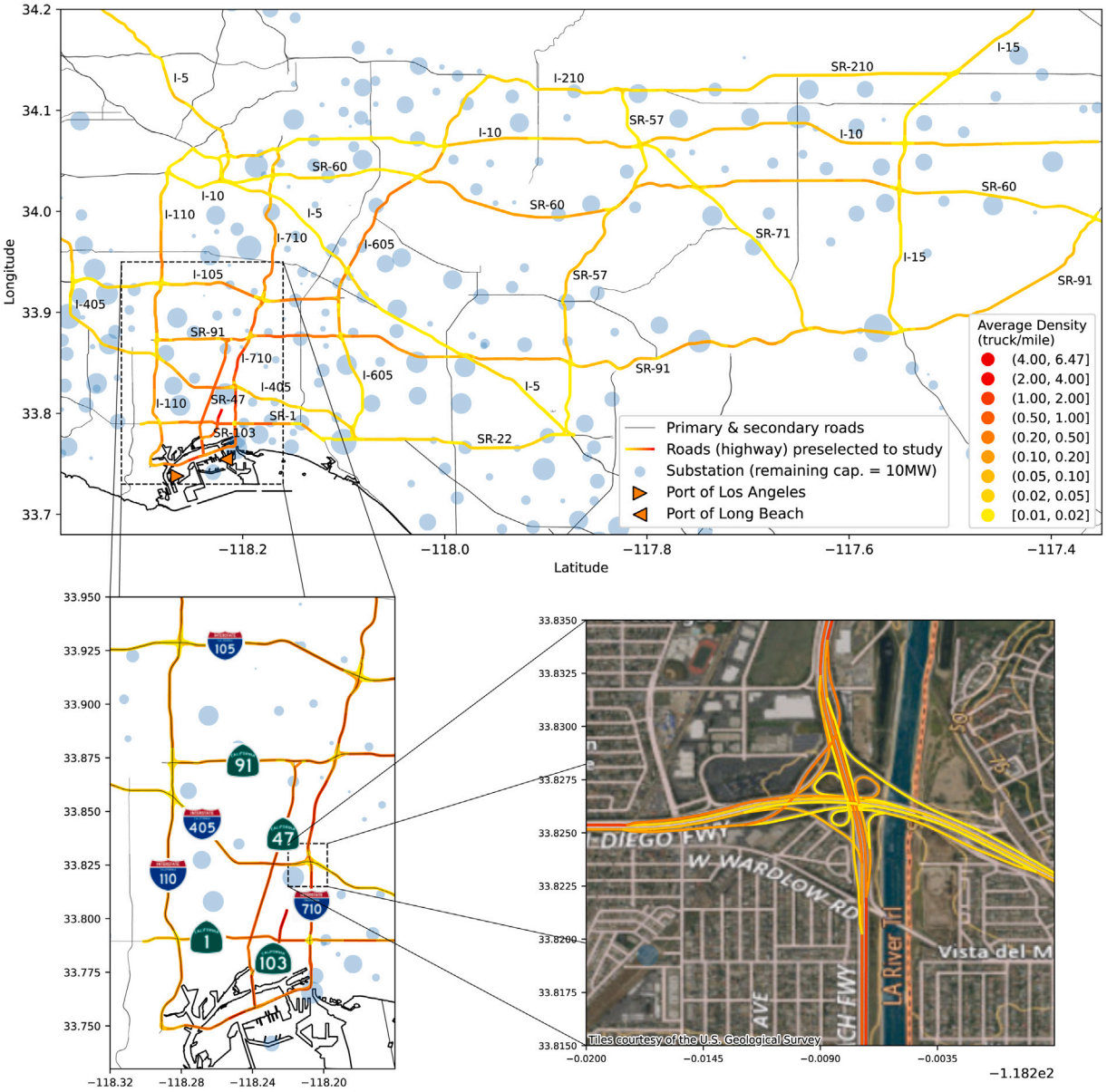

Fig. 5. Overview of the study area. Top: Highway network of the Greater Los Angeles area with annual-averaged drayage truck traffic density and the locations of electrical substations whose size is proportional to the remaining load hosting capacities; Bottom-left: A zoom-in view of the port area and the specific highways; Bottom-right: A zoom-in view of the intersection of I-405 and I-710.

we refer to the resultant segments as "raw" segments. The raw segments obtained from the trajectories of different trucks are then compiled into a single file. Ultimately, we merge these raw segments into our desired length (one mile), thereby creating the final segments for the study. As this process is intricate, we provide a detailed explanation in Appendix C for interested readers.

5.2.2. From GPS data to dwell time statistics

After establishing the road segments, we also receive the entry and exit time points for each raw segment each time a truck traverses this segment. As these raw segments are merged into the final road segments, these sequences of entry and exit times are transferred over as well. We developed an algorithm to calculate the number of trucks on a road segment at different times. From this, we can derive the truck dwell time statistics $t_i(n), \forall i \in I$, which serve as input to (1). Similar to Section 5.2.1, more details can be found in Appendix C for interested readers. While the use of historical GPS data in illustrating the deployment of DWCLs primarily serves as an example, we recognize its limitations due to potential changes in freight activities. Future applications of our study should certainly utilize more recent GPS data, along with traffic growth projections, to ensure accuracy and relevance.

5.3. Electrical substations

Southern California Edison (SCE) is the major electric utility provider in the Greater Los Angeles area. Publicly available information provides the details about their electrical distribution substations, including estimated remaining load capacities for each substation [50]. In this study, we incorporate the substations within our defined study area, resulting in a total of 255 substations. These substations' locations are depicted in Fig. 5, with the size of each circle corresponding to the respective substation's remaining load hosting capacity. A summarized histogram of the remaining load hosting capacities and the count of substations is shown in Fig. 6. It should be noted that while this study does not include the construction of new substations, such additions could be easily accommodated once candidate locations are provided.

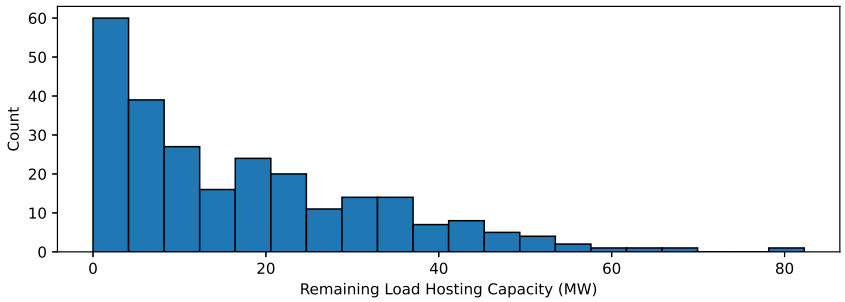

Fig. 6. Histogram of the remaining load hosting capacities of electrical substations within the study area.

Table 2
List of Initial Investments, Lifespans, and the Amortized Annual Costs.

Asset	Initial investment P	Lifespan n (years)	Annual cost A
DWCL, include:			
•Initial deployment	$5,310,000/mile	25	$584,992/mile
•Annual maintenance	$79,650/mile	–	$79,650/mile
Step-down transformers	$200,000/MW	25	$22,034/MW
Distribution lines	$1,200,000/mile	30	$127,295/mile
Substation upgrade, include:			
•Fixed	$4,600,000/upgrade	25	$506,773/upgrade
•Variable	$200,000/MW	25	$22,034/MW
Line losses	–	–	$100/MWh

5.4. Cost of assets

The initial investment for DWCL deployment is derived from Konstantinou et al. [20], where the estimated cost of DWCL deployment ranges from 6.32 to 6.55 million $/mile. This estimation encompasses the charging system, civil infrastructure, and power distribution system. Since our study provides a more localized and detailed examination of the power distribution system's cost, we subtract the general estimated cost of the power system from the total, resulting in a revised DWCL deployment cost of $5.31 million/mile. The annual maintenance cost of the DWCLs is assumed to be 1.5% of the capital investment [20]. The cost of pairing step-down transformers, including necessary make-ready investments like wires, conduits, and meters, is estimated to be $0.20 million/MW, as per Nelder and Rogers [51]. The cost of distribution lines varies widely, depending on a number of factors such as land acquisition requirements, voltage ratings, and whether the lines are overhead or underground. Based on information in MISO [52] and consultations with a local utility company, we estimate the cost of distribution lines to be $1.20 million/mile. Building distribution lines along roads is generally less expensive than over land [48], leading us to estimate a discount factor λ of 0.5. The cost of substation upgrades, including a standard 28MVA transformer and necessary capacitor banks, is estimated to be $4.60 million/upgrade, again drawing from MISO [52] and consultations with the local utility. We also estimate the variable cost of substation upgrades to be $0.20 million/MW, aligning with the cost of pairing transformers with DWCLs. The cost of line losses is based on local wholesale electricity prices, estimated at $100 per MWh.

The costs of assets will be amortized annually based on a specified interest rate and the hardware's expected lifespan. The annual cost of an asset is calculated based on the standard $(A|P,r,n)$ factors from engineering economics [53], where A denotes the annual cost, r is the discount rate (assumed to be 10% [54]), n is the lifespan of the asset (in years), and P is the initial investment in the asset. By substituting P and n for different assets, we obtain their amortized annual cost as listed in Table 2:

In addition to the hardware-related costs, congestion costs represent a significant external cost during the construction and maintenance of DWCLs. Aligning DWCL deployment with road pavement replacement or maintenance can mitigate or eliminate these costs. However, it is also crucial to consider scenarios where congestion costs apply. Considering congestion costs ensures a more realistic assessment of the overall economic impact of DWCL deployment, particularly in high-traffic areas where lane closures can significantly disrupt traffic flow. For this purpose, we have adopted a streamlined method to estimate the congestion cost associated with single-lane closures for each segment, as detailed in Appendix D. A comparative study, analyzing the impact with consideration of congestion costs, is presented in Section 7.4.

6. Solution methodology

Solving the proposed optimization problem directly can be challenging. The complexity primarily stems from two factors: (1) the combinatorial nature of segments (x_i) and SCSs (y_j), and (2) the potential long chain of road connections $(\widehat{p^{road}_{i'i}})$, i.e. a chain of road connections can span numerous segments until the line current limit is reached. These challenges can inhibit the solver's efficiency in finding optimal solutions. In fact, by solving the problem directly, we have yet to obtain a feasible solution after running the solver for several days (solved with Gurobi on a desktop machine with 40 Intel Xeon Silver 4210 2.20 GHz CPUs). Taking inspiration from Marcucci and Tedrake [55] and Miltenberger [56] that a "warm start" solution can expedite the solving process, we designed a comprehensive procedure that can significantly accelerate the solution process, as illustrated in Fig. 7. The procedure starts with generating high-quality feasible solutions by controlling the sources of complexity, and eventually attaining the near-optimal solutions with a MIP gap of less than 1%. Initially, we commence with a low-budget scenario where B = $15 million/year. The step-by-step process is as follows:

- Step 1: To start with, we solve the problem by temporarily removing the complexity introduced by road connections, which means we set $\widehat{p^{road}_{i'i}} = 0, \forall i \in I, i' \in N_i$. The result from this step provides a feasible solution to the original problem. However, this solution does not utilize low-cost road distribution lines, implying that the same budget could potentially be allocated more efficiently. We aim to address this in the subsequent step.

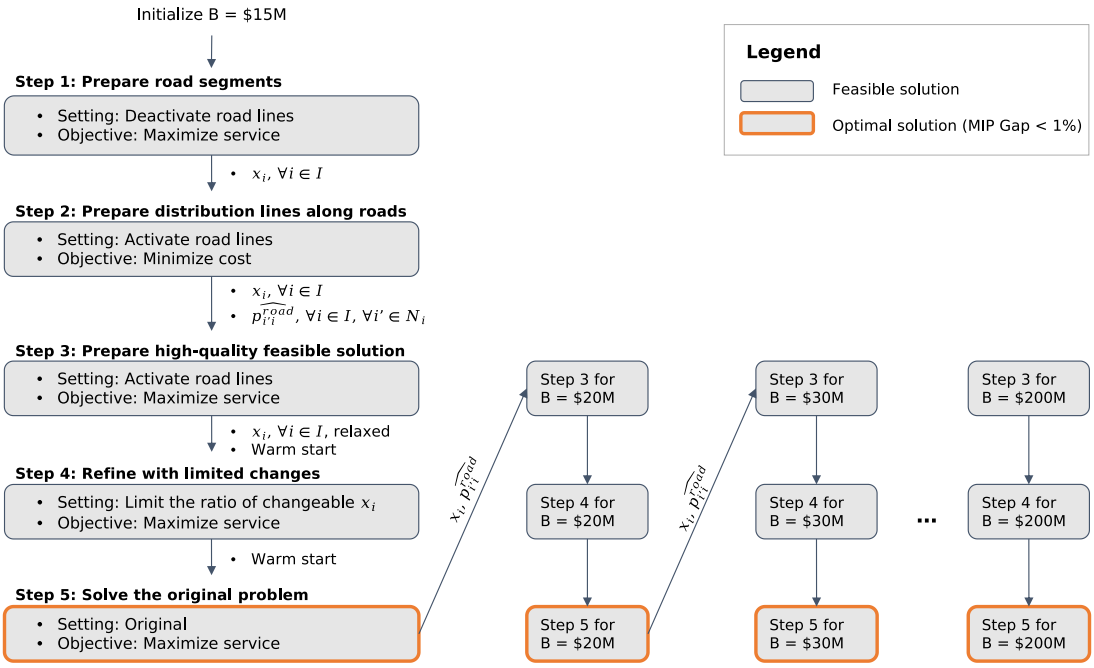

Fig. 7. Complete workflow of the solution method.

- Step 2: In this step, we activate the use of road distribution lines. To manage the complexity introduced by the combinatorial nature of segments and SCSs, we incorporate "soft" constraints based on the segments identified in Step 1 (i.e., we set $x_i \geq x_i^{pre}, \forall i \in I$, where x_i^{pre} are the solutions derived from Step 1). We then solve the problem with the objective of minimizing costs, as defined in the left-hand side of (24), while ensuring that the annual electricity supplied does not drop below that obtained in Step 1. Notably, the solution obtained in this step represents a feasible solution at a lower budget than the targeted $B = \$15$ million/year.
- Step 3: This step is designed to obtain a high-quality feasible solution at the targeted budget level. Specifically, in Step 3, we inherit the solution from Step 2 and set soft constraints again: $x_i \geq x_i^{pre}, \forall i \in I$ and $\widehat{p_{i'i}^{road}} \geq \widehat{p_{i'i}^{road,pre}}, \forall i \in I, i' \in N_i$, where x_i^{pre} and $\widehat{p_{i'i}^{road,pre}}$ are the solutions from Step 2. By optimizing the problem with the objective of maximizing annual electricity supplied, and reinstating the budget constraint (24) as in Step 1, we attain a high-quality feasible solution for the desired budget. Although this solution does not meet the targeted optimality level, it provides a firm foundation for subsequent optimization steps.
- Step 4: Here, we remove the soft constraints tied to $\widehat{p_{i'i}^{road}}$, and for x_i, we substitute its associated soft constraints with a set of less rigid constraints. This means that rather than mandating all x_i to be greater or equal to x_i^{pre}, we allow a certain ratio of x_i to alter. This modification is achieved through the following constraints:

$$x_i \geq \alpha_i \cdot x_i^{pre}, \forall i \in I, \tag{25}$$

$$\sum_{i \in I} \alpha_i \geq (1 - R) \sum_{i \in I} x_i^{pre}, \tag{26}$$

where x_i^{pre} is the solution from Step 3 and R is the ratio of allowed changeable x_i; we set $R = 0.1$. Constraints (25) and (26) imply that there is a high likelihood to find a near-optimal solution by modifying only 10% of the previous solution x_i^{pre} from Step 3. The narrowing of search space can significantly speed up the solving process. The rest part of the solution from Step 3 will also be utilized to warm start the problem in Step 4.

- Step 5: Finally, we apply the solution from Step 4 to warm start the original problem. With this high-quality feasible solution acquired after Steps 1–4, we can efficiently obtain the desired near-optimal solution (MIP gap < 1%) with a solver time of fewer than two hours.

Following the same procedure, the optimal solution for the budget of $B = \$15$ million/year can serve as a feasible solution for higher budget scenarios — We iterate through Steps 3–5 to find the optimal solutions corresponding to these higher budget scenarios.

7. Results and discussion

This section explores the cost–benefit analysis, sensitivity analysis, and expansion progress of the DWCL project. In the cost–benefit analysis, we examine DWCL length, annual electricity supplied, road and land line lengths, and substation utilization/upgrade across various budgets. In the sensitivity analysis, we further evaluate how the annual electricity supplied is impacted by electric truck penetration rates, unit-length power capacity, and discount rates. After that, the geographical expansion of DWCLs under different budget thresholds is visually presented, highlighting developmental stages and strategic decisions of DWCL deployment. Lastly, we analyze the impact of congestion costs on the deployment of DWCLs, focusing on how the inclusion of the congestion costs affects the overall objectives and the geographical expansion of DWCLs.

7.1. Cost–benefit analysis

A comprehensive cost–benefit analysis is carried out in this section. The primary goal is to understand the variations in annual electricity supplied at different budget thresholds and the allocation of resources across various sectors. To achieve this, we employ the solution procedure outlined in Section 6 and report the findings for annual budgets ranging from $20 million to $200 million, increased incrementally by $10 million. A complete set of results is depicted in Fig. 8. Noteworthy findings include:

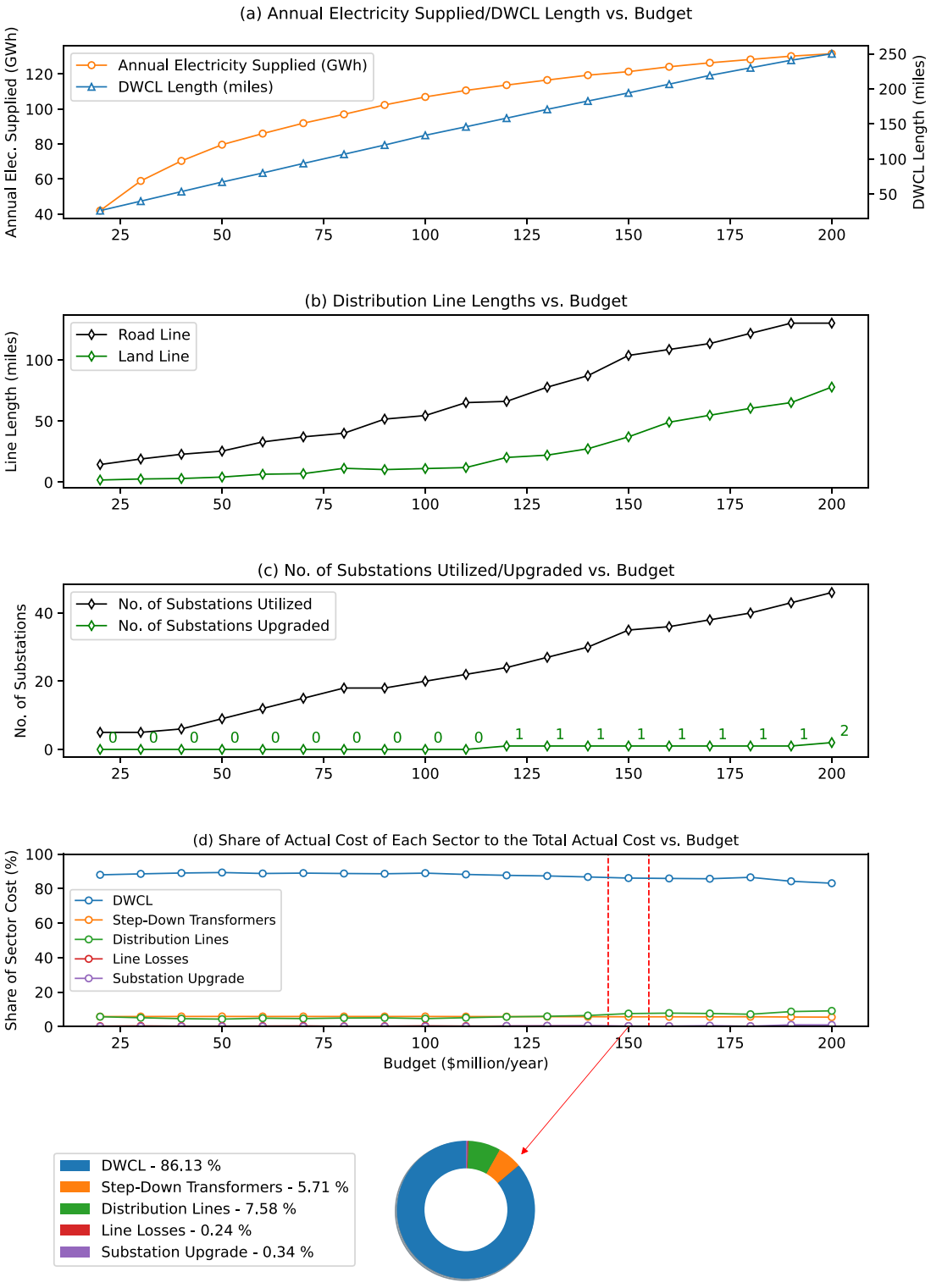

Fig. 8. Overview of the planning results and resource allocation schemes under various budget thresholds.

- The annual electricity supplied and DWCL lengths at varying budget thresholds are reported in Fig. 8(a). While the total DWCL length is observed to increase linearly with the budget, the growth of annual electricity supplied slows down gradually. This reduced rate of increase in annual electricity supplied indicates that DWCL coverage is extending to less busy highways. This means that policymakers and charging infrastructure developers should make appropriate investment decisions by comparing the costs and benefits of DWCLs against alternative charging options.
- Fig. 8(b) illustrates the lengths of road and land distribution lines. The distribution lines along roads are observed to be longer than those across land. This is due to the well-established right-of-way along roads, making it more cost-effective to build distribution lines there. As a result, DWCLs typically favor power supply from

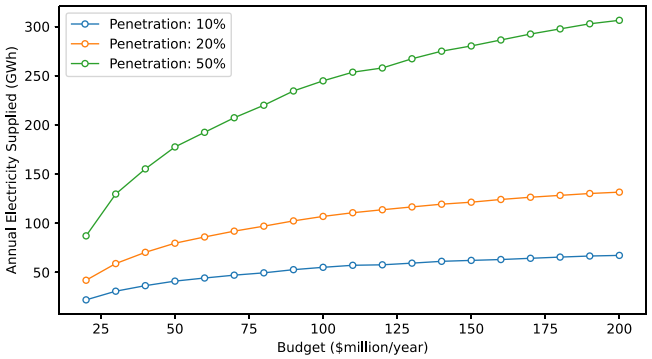

Fig. 9. Variations of annual electricity supplied under different electric truck penetration rates and budget thresholds.

connections with nearby segments rather than direct connections with the substations, as long as the line current does not exceed the limit and the benefits outweigh the extra line losses. An increase in the length of land lines is significant once the budget exceeds $110 million/year. This is due to the DWCLs extending beyond the port area, which is characterized by a less dense distribution of substations. Consequently, this requires the establishment of longer land lines to connect DWCLs with substations.

- The number of substations utilized and upgraded are depicted in Fig. 8(c). With the default 2 MW/mile power capacity design, the existing substations can satisfy the power demand from DWCLs without upgrades in most cases. An upgrade is triggered only when the development scale reaches $120 million/year. This can be attributed to the expansion of the DWCLs into areas with fewer choices of substations, where it becomes more economical to upgrade an existing substation, despite the associated high costs.
- The cost distribution is reported in Fig. 8(d). The majority of the total expenditure is allocated to DWCLs, followed by distribution lines and step-down transformers. As the project scale (i.e., budget) expands, the share of DWCL cost decreases, while the share of distribution line cost increases. This trend is again due to the expansion of the DWCL into areas with fewer substations, necessitating longer lines for connections between DWCLs and more distant substations. Detailed cost information for a $150 million/year budget is provided beneath Fig. 8(d). It shows that the costs of line losses and substation upgrades are relatively insignificant given the default 2 MW/mile power capacity design.

In summary, the analysis compares the growth rates of annual electricity supplied and DWCL length under increasing budget thresholds and explains the reduced growth rate of annual electricity supplied. The distribution lines along roads are typically longer due to their cost-effectiveness, and an increase in land line length is notable as budgets exceed $110 million/year, due to DWCLs reaching areas with fewer substations. Most existing substations can accommodate the power demand without upgrades until the project scale reaches $120 million/year. Furthermore, as the project scale increases, the share of cost allocated to DWCLs decreases, while that of distribution lines rises. Detailed cost information reveals relatively minor costs for line losses and substation upgrades given the default 2 MW/mile power capacity design.

7.2. Sensitivity analysis

7.2.1. Electric truck penetration rates

A major concern that remains with the DWCL project is whether the current design can adequately support the charging demands of electric trucks as their penetration rates increase. To address this question, we examine the annual electricity supplied at different electric truck penetration rates. Remember that our dataset of 7,150 drayage trucks represents 20% of the total drayage truck population, and the dwell time statistics at each segment, $t_n(i)$, are derived from sequences of entries and exits. We obtain $t_n(i), \forall i \in I$ for a lower penetration case (10%) through randomly sub-sampling half of the entry and exit sequences, and for a higher penetration case (50%) through randomly duplicating samples to create 2.5 times more sequences. We then solve the optimization problems under different budget thresholds and present the results in Fig. 9.

As depicted in Fig. 9, the annual electricity supplied tends to plateau sooner when the penetration rate is low. Conversely, with a 50% penetration rate, the annual electricity supplied continues to show strong growth even at high budget thresholds. At a budget level of $100 million/year, the annual electricity supplied for 10%, 20%, and 50% penetration rates is 55.1 GWh, 106.9 GWh, and 244.8 GWh, respectively. The annual electricity supplied at 20% and 50% penetration rates is approximately 1.9 and 4.4 times higher than that at a 10% penetration rate, nearly mirroring the ratio of penetration rates. The fact that the growth of annual electricity supplied aligns closely with the increase in penetration rates indicates that few road segments regularly reach the maximum charging power and subsequently become capped. In other words, the current DWCL power capacity design appears to be sufficient to handle the demand for future electric trucks. If penetration rates continue to grow beyond 50%, our model can easily support adding more connections with substations and/or upgrading existing substations to meet demand.

7.2.2. Unit-length power capacity

Another aspect that can significantly influence annual electricity supplied is the power capacity designed for the DWCLs. A design with a higher power capacity per unit length (ρ) is more likely to accommodate peak demands. However, this comes with the trade-off of requiring transformers with higher capacities and potential upgrades to substations. To understand the optimal selection of power capacity, we study scenarios with varying power capacities, specifically with $\rho = 1$, 2, and 4 MW/mile, as presented in Fig. 10. The selection of candidate power capacities is inspired by Trinko et al. [57]. All results are based on the default penetration rate of 20%. Specifically, we compare the growth of annual electricity supplied and DWCL length across different budget thresholds.

Fig. 10(a) illustrates that a design incorporating $\rho = 4$MW/mile delivers a similar level of annual electricity supplied as one with $\rho = 2$MW/mile, up until the budget hits the $50 million/year mark. Beyond this threshold, the annual electricity supplied with $\rho = 4$MW/mile begins to lag behind those of $\rho = 2$MW/mile, largely due to the increased resource allocation required for connections with additional substations and the necessity for substation upgrades to support the higher power capacity design. This notion is further reinforced by Fig. 10(b), which demonstrates that a longer stretch of DWCLs can be built using $\rho = 2$MW/mile, compared to $\rho = 4$MW/mile, primarily due to the budget savings achievable from the less demand of power systems.

On the other hand, although a design with $\rho = 1$MW/mile allows for the construction of longer DWCLs compared with $\rho = 2$MW/mile, its annual electricity supplied remains below that of $\rho = 2$MW/mile. This is due to the fact that peak demands cannot be fully met with only $\rho = 1$MW/mile. Interestingly, by comparing the cases with $\rho = 1$MW/mile and $\rho = 4$MW/mile, although the former's annual electricity supplied is lower, it appears poised to overtake the latter at and beyond the budget threshold of $200 million/year. This is potentially because, as DWCLs extend to less busy highways with reduced charging demand, the advantage offered by a high power capacity starts to diminish. Overall, at a penetration level of 20%, $\rho = 2$MW/mile is found to be a more competitive design compared to 1 or 4MW/mile.

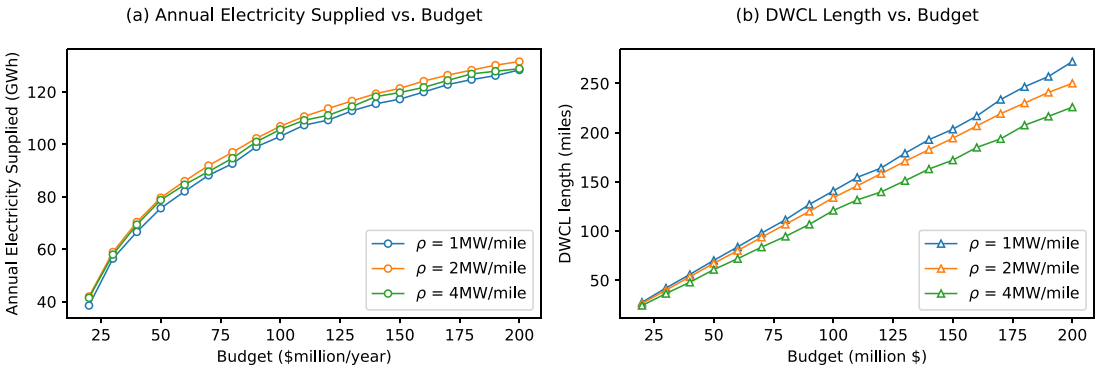

Fig. 10. (a) The annual electricity supplied under designs of $\rho = 1$, 2, and 4 MW/mile at varying budget thresholds. (b) The corresponding DWCL lengths achievable under these designs.

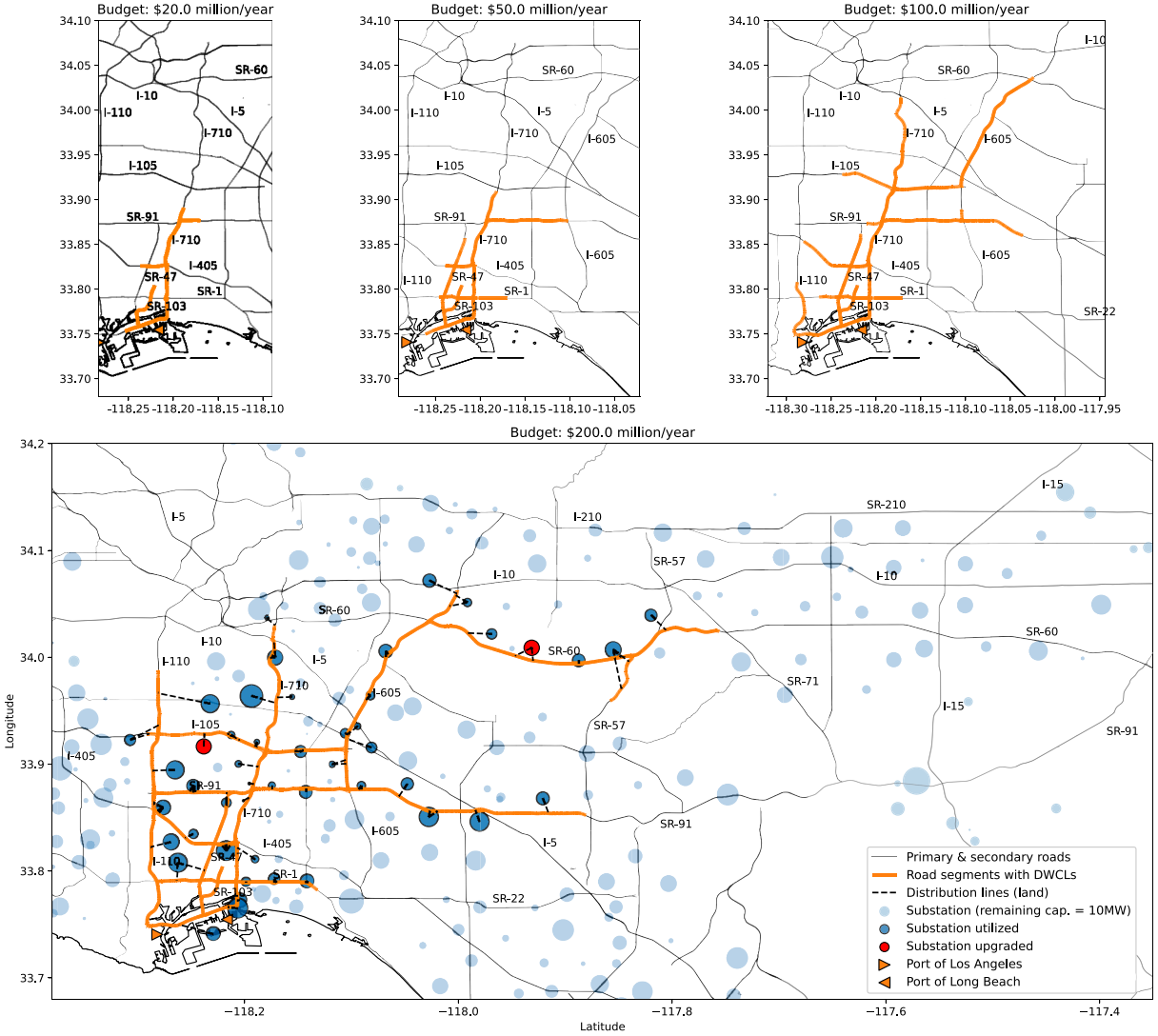

Fig. 11. Expansion of DWCLs with the increase of budget thresholds.

7.2.3. Discount rates

In this subsection, we examine the sensitivity of our results to variations in discount rates. This analysis is particularly important for infrastructure projects like DWCLs, characterized by significant upfront costs and benefits that accumulate over an extended period. In addition to the base case with a 10% discount rate, we explore two additional discount rates of 5% and 15%, as discussed in Fripp [54], to represent scenarios with lower and higher discount rates, respectively. The outcomes of these three discount rates are shown in Fig. 12. The impact of the discount rate is notably significant on both the annual electricity supply and the achievable lengths of DWCL under various budget scenarios. As the budget increases and DWCLs are extended

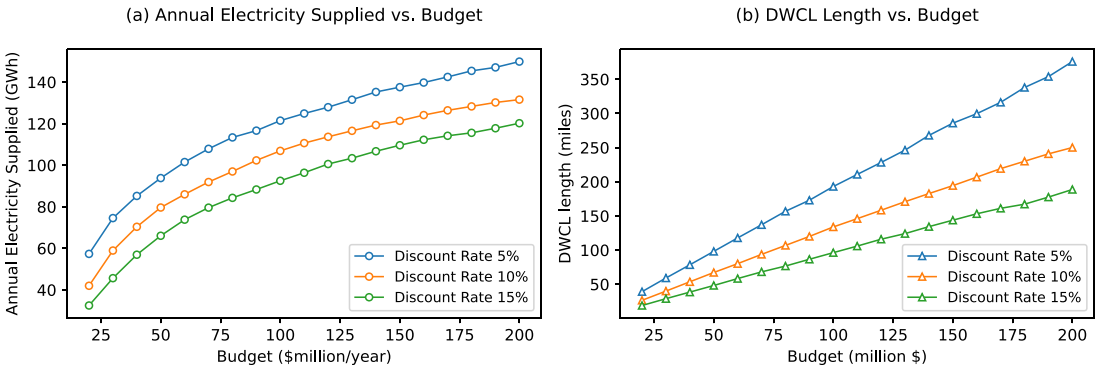

Fig. 12. (a) The annual electricity supplied under discount rates of 5%, 10%, and 15% at varying budget thresholds. (b) The corresponding DWCL lengths achievable under these discount rates.

to less busy areas, the influence of the discount rate becomes more pronounced on the DWCL length than on the electricity supply. For instance, at an annual budget of $200 million, the electricity supply varies from 149.9 GWh at a 5% discount rate to 120.2 GWh at a 15% rate, representing a variation range of +13.9% to −8.6% compared with the base case (131.6 GWh). In contrast, the variation in DWCL length for the same budget level shows a more substantial range of +50.3% to −24.6% compared with the base case (250.1 miles). The variation in results driven by different discount rates highlights their critical role in the economic assessment of DWCLs.

7.3. Development expansion progress

In this subsection, we visually present and analyze the geographical expansion of DWCLs under increasing budget thresholds, as shown in Fig. 11. At a low budget threshold of $20 million/year, initial DWCL deployment emerges from the port area, a region characterized by high drayage truck density. The abundance of substations around the Port of Long Beach, most with sufficient remaining load hosting capacities, facilitate this deployment. As the budget increases to $50 million/year, DWCLs' footprint radiates north and east from the port area. Because of a relatively low density of substations, the coverage further extends westward until the budget reaches $100 million/year. The bottom of Fig. 11 showcases utilized/upgraded substations and land distribution lines for the $200 million/year case, alongside DWCLs. A dense distribution of substations can be observed around the port area, but the density gradually reduces as we move eastwards. Two highlighted substations marked in red for upgrades are also identifiable, crucial for continuing DWCL expansion in areas where the choice of substations is limited.

7.4. Impact of congestion costs

In this subsection, we analyze the impact of congestion costs. We particularly focus on how the inclusion of the congestion costs affects the overall objectives (i.e. the annual electricity supplied) and the geographical expansion of DWCLs. The congestion costs were estimated based on the annual average daily traffic for specific road segments, considering speed reductions due to one-lane closure, as outlined in Appendix D. The congestion costs are then added to the hardware and maintenance costs of the DWCLs and amortized over the DWCLs' lifespan.

Our comparative analysis, shown in Fig. 13, examines the differences in annual electricity supplied and DWCL expansion when considering the base case against a scenario that includes additional congestion costs. The base case represents a 20% electric truck penetration and a DWCL design with a 2 MW/mile power capacity, but without considering congestion costs. As Figs. 13(a) and (b) illustrate, the same budget yields less output when congestion costs are included. For instance, with an annual budget of $200 million, the electricity supply drops from 131.6 GWh in the base case to 104.7 GWh – a 20.4% reduction – when congestion costs are considered. Moreover, the DWCL length reduces from 250.1 miles to 129.8 miles, marking a 48.1% decrease. Figs. 13(a) and (b) underscore the significant impact of congestion costs in DWCL planning. However, they also reveal that by prioritizing high-demand road segments, the reduction in annual electricity supply is comparatively smaller than the reduction in DWCL length.

Fig. 14 maps the spatial shift in DWCL deployment under the same $200 million annual budget. Notably, expansions on SR-60 and SR-91 are curtailed due to budget constraints. The port area, with its heavy drayage truck traffic, remains a priority. However, a notable gap emerges around the I-105 and I-605 interchange, attributed to the relatively high congestion costs. In summary, this spatial analysis provides a more detailed view of the substantial influence of congestion costs. It is noteworthy that synchronizing DWCL construction with road pavement replacement and maintenance activities could yield outcomes more aligned with the base case scenario. Achieving the synchronization requires a spatio-temporal modeling approach in future studies, focusing not only on optimizing the locations but also on the timing of implementation.

8. Conclusion

Dynamic wireless charging lanes (DWCLs) are a promising charging option that has great potential to facilitate the electrification of heavy-duty drayage trucks. The deployment of DWCLs and the subsequent electrification of drayage trucks would contribute to both immediate mitigations of urban air pollution and long-term decarbonization goals. This study established an optimization framework to address the pivotal issues in DWCL deployment for drayage trucks, including identifying optimal locations for DWCLs, connecting them to the grid, and determining the necessity for power system upgrades to meet the additional demand. Large-scale GPS trajectory data of drayage trucks is utilized to provide important inputs to the framework, including the road segments and the truck dwell time statistics. Inspired by warm start strategies, a tailored solution method workflow is developed to overcome the high complexity of the original problem. A case study is then conducted focusing on the Greater Los Angeles area, home to two of the world's busiest seaports. The case study helps determine the strategic expansion plan of DWCLs around the targeted area with a complete cost–benefit analysis under different budget scenarios. The optimization framework and analysis methodologies can be easily extended to other areas as well.

However, this study has its limitations. First, while past GPS data effectively illustrates DWCL deployment, it may not fully capture potential shifts in freight activities. Future applications should incorporate

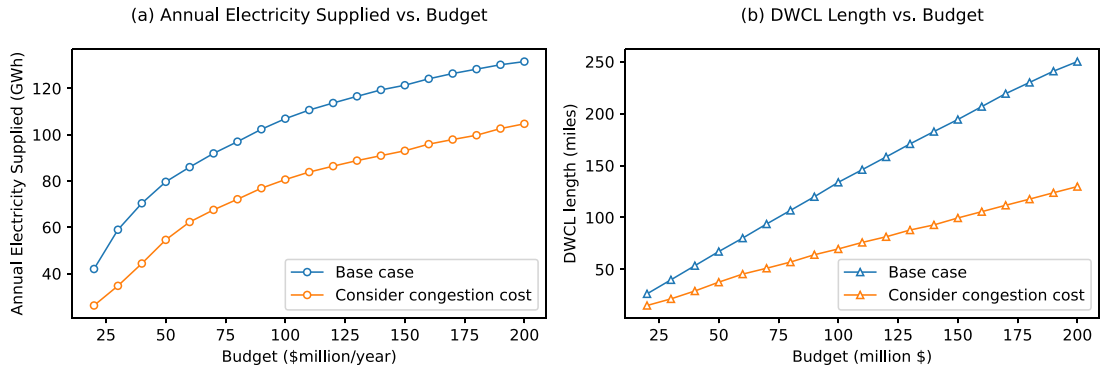

Fig. 13. (a) The annual electricity supplied under the base case and the case considering congestion costs. (b) The corresponding DWCL lengths achievable under these two cases.

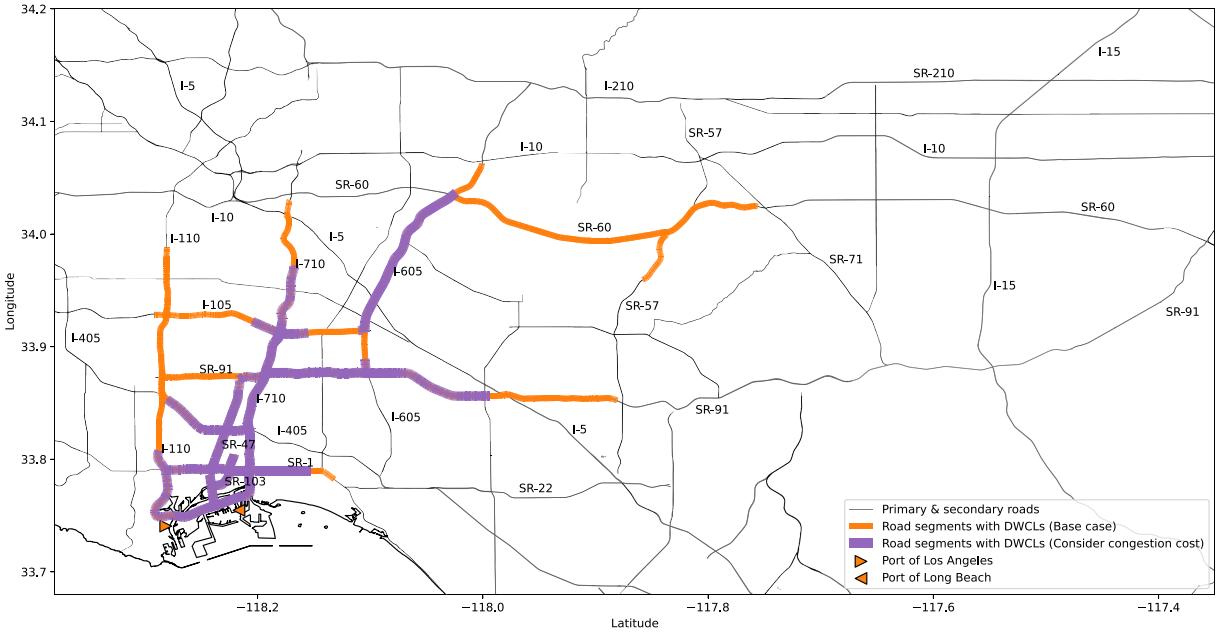

Fig. 14. Comparative spatial deployment of DWCLs with a $200 million annual budget: Base case and congestion cost consideration.

recent GPS data and traffic growth projections for better accuracy and relevance. Second, the assumption that substations' remaining power capacity can be entirely allocated to DWCLs is overly optimistic, as this capacity is shared with other loads, including residential and industrial. A more realistic approach would account for the projected growth of these other loads, likely resulting in a greater need for substation upgrades. Nonetheless, our current analysis provides a foundational understanding that can be enhanced and refined with updated data.

It is worth mentioning that in this study, the objective is to maximize the total annual electricity supplied by DWCLs, while neglecting the time of the day at which the electricity is supplied. However, the timing of charging has implications for the carbon intensity of electricity. Charging during periods of dominant renewable energy would allow electric trucks' batteries to absorb excess "green" electricity, reducing the demand for stationary energy storage, and achieving more effective GHG reduction than during periods of fossil-fueled generation dominance. Therefore, considering the time-varying mix of power generation in future planning is a promising direction.

Moreover, the timing of DWCL deployment is also crucial, calling for a spatio-temporal model that aligns DWCL construction with road pavement replacement and maintenance schedules. Additionally, DWCLs' ability to reduce the required battery capacity for electric trucks and lower the adoption barrier further highlights their potential. Addressing these aspects necessitates innovative ideas and modeling approaches, aligning with regional goals for electric truck adoption.

CRediT authorship contribution statement

Zuzhao Ye: Writing – original draft, Visualization, Validation, Software, Methodology, Data curation, Conceptualization. **Mikhail A. Bragin:** Writing – review & editing, Software, Methodology. **Nanpeng Yu:** Writing – review & editing, Supervision, Resources, Project administration, Methodology, Data curation, Conceptualization. **Ran Wei:** Writing – review & editing, Supervision, Resources, Methodology, Funding acquisition, Data curation, Conceptualization.

Declaration of competing interest

The authors declare the following financial interests/personal relationships which may be considered as potential competing interests: Ran Wei reports financial support was provided by University of California Institute of Transportation Studies.

Data availability

Data will be made available on request.

Acknowledgments

This study was made possible with funding received by the University of California Institute of Transportation Studies from the State of California through the Public Transportation Account and the Road Repair and Accountability Act of 2017, United States (Senate Bill 1). This document is disseminated under the sponsorship of the State of California in the interest of information exchange and does not necessarily reflect the official views or policies of the State of California.

Appendix A. Recursive algorithm to obtain set J of all SCSs

Algorithm 1 is developed to find the set J that consists of all possible SCSs in a recursive way. The basic idea is that we start from a segment and explore its adjacent segments along the direction of traffic until the minimal contiguous length is reached. The algorithm relies on the input of $I_i^{next}, \forall i \in I$, which is the set of adjacent segments of segment i along the direction of traffic. For instance, on a straight road, segment i_0 would have one adjacent segment i_1 opposite the traffic direction and another i_2 along the traffic direction. In this case, $I_{i_0}^{next} = \{i_2\}$. For a segment i_0 positioned before an intersection or a ramp, $I_{i_0}^{next}$ would include multiple segments. After the completion of Algorithm 1, we obtain 9,097 SCSs in total.

Algorithm 1: The recursive algorithm to obtain set J of all SCSs

Input : $I_i^{next}, \forall i \in I$, the set of adjacent segments of segment i along the direction of traffic.
Output: J, set of all possible SCSs.

```
// Define the recursive base function.
def findNextSegment(i: int, SCS^current: [list], L^cum: float):
    if I_i^next = ∅ then
        return;
    end
    for i' ∈ I_i^next do
        if i' ∈ SCS^current then
            Skip the following procedure and continue;
        end
        SCS^temp ← copy(SCS^current);
        SCS^temp ← SCS^temp ∪ {i'};
        L^new = L^cum + l_i';
        if L^new ≥ L^thres then
            J ← J ∪ {SCS^temp};
        else
            findNextSegment(i', SCS^temp, L^new);
        end
    end

// Running the recursive base function starting
   from every segment in I.
Initialize global empty set J ← ∅ to store all SCSs;
Initialize global threshold length L^thres = 10 miles;
for i ∈ I do
    Initialize SCS^current ← ∅;
    findNextSegment(i, SCS^current, l_i);
end
return J
```

Appendix B. Linearization of conditional constraints

In this subsection, we introduce how the conditional constraints (12) and (13) are linearized before they can be handled by the solver. For (12), we introduce the following Eqs. (27) and (28) to replace it. G is a relatively large number. These two equations work in the following ways to ensure (12) is satisfied: (1) When $p_{i'i}^{road} \neq 0$, it requires $\widehat{p_{i'i}^{road}} \neq 0$ as well, i.e. $\widehat{p_{i'i}^{road}} = 1$; (2) When $p_{i'i}^{road} = 0$, $\widehat{p_{i'i}^{road}}$ can be either 0 or not based on (27)–(28), however, the solver will assign $\widehat{p_{i'i}^{road}} = 0$ eventually as it implies additional cost in (24).

$$p_{i'i}^{road} \leq G\widehat{p_{i'i}^{road}} \tag{27}$$

$$p_{i'i}^{road} \geq -G\widehat{p_{i'i}^{road}} \tag{28}$$

Similarly, for (12), we introduce the following Eq. (29) to replace it. When $p_{ki}^{land} \neq 0$, it requires $\widehat{p_{ki}^{land}} \neq 0$ as well, i.e. $\widehat{p_{ki}^{land}} = 1$; When $p_{ki}^{land} = 0$, the solver will assign $\widehat{p_{ki}^{land}} = 0$ to save budget, similar to the mechanism of $\widehat{p_{i'i}^{road}}$.

$$p_{ki}^{land} \leq G\widehat{p_{ki}^{land}} \tag{29}$$

Appendix C. GPS data processing

C.1. From GPS data to road segments

The derivation of road segments from GPS data involves a set of seven steps as outlined in Fig. 15. Among the seven steps, Steps 1 and 2 were carried out using the Python API of ArcGIS (ArcPy) [58], while Steps 3–7 were accomplished through custom algorithms developed in Python. The details of each step is as follows:

- Step 1: The first step involves projecting the original GPS points onto the closest road network when they fall outside of the road network due to measurement errors. This process, also known as "Snap" in ArcGIS, ensures that the GPS points align with the road network.
- Step 2: The ArcGIS network analyst toolset [49] is utilized to determine the route with minimum travel time between two consecutive points. Each route consists of a set of internal points that reflect the precise route.
- Step 3: In this step, the internal points are extracted from the routes obtained in Step 2.
- Step 4: The snapped GPS points are removed, and small segments are created by connecting the leading and trailing points in sequence. These small segments, referred to as raw segments, need further processing to produce the final segments used in the model. The purpose of removing the snapped GPS points, which are unique to individual trucks, is to ensure consistency of internal points when different trucks traverse the same route.
- Step 5: To create a set of unique raw segments, this step groups together identical raw segments from different passes. These passes can be from the same truck but in different orders, or from different trucks.
- Step 6: A highway buffer of 164 ft (50 m) is employed to filter raw segments within the buffer and the rest is discarded. Note that there are still a limited number of non-highway raw segments that fall within the buffer, and we manually eliminated all non-highway segments and only kept the highway segments. Upon completing Step 6, we obtain I^{raw}, which represents the set of raw segments.
- Step 7: Since raw segments are typically very short (can be as small as a few feet), we merge them into longer segments to reduce the complexity of the model. Hence, in Step 7, the raw segments are merged into the final segments used in the model following Algorithm 2, targeting a length of 1 mile. Further details regarding Step 7 will be provided in the rest of this section.

We will now proceed with "growing" the raw segments into the final 1-mile segments according to Algorithm 2. In the initial stage, we extract three types of segments from I^{raw}: starting, ending, and isolated (S/E/ISO). As illustrated in Fig. 16, the S or E-type segments should fall into the following two categories:

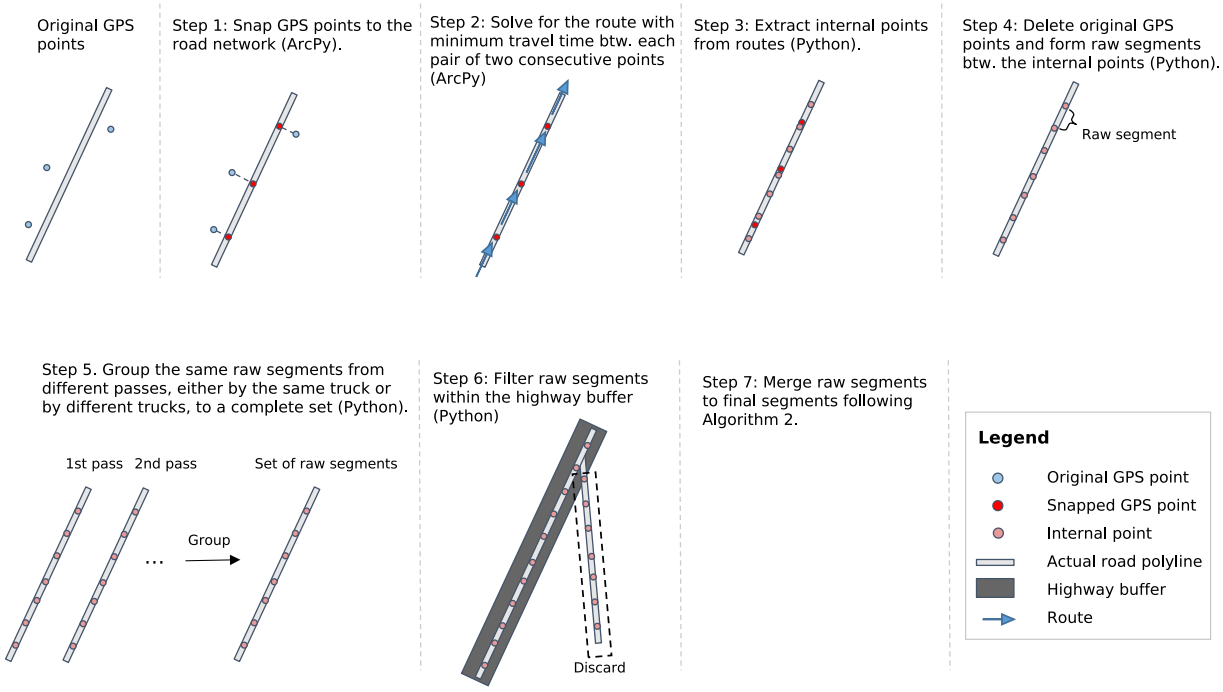

Fig. 15. Procedures to derive road segments from GPS data.

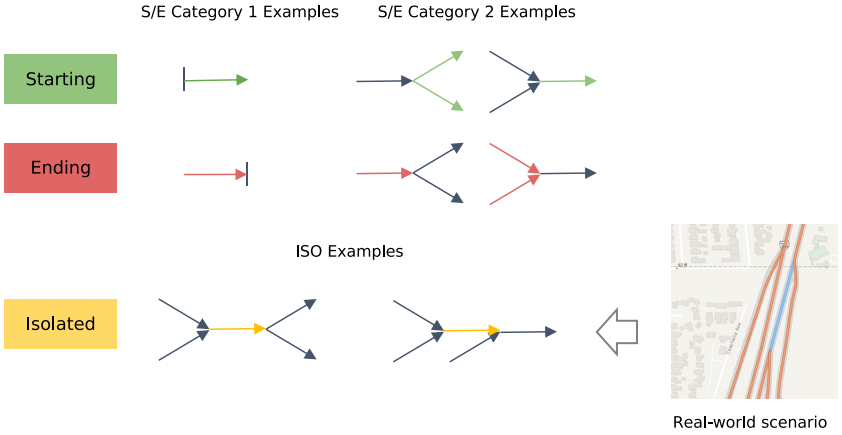

Fig. 16. Examples of starting/ending/isolated (S/E/ISO) raw segments.

- Category 1: Raw segments at road ends or study area boundaries:
  - Starting: Raw segments without any adjacent raw segments in the opposite direction of traffic.
  - Ending: Raw segments without any adjacent raw segments in the direction of traffic.
- Category 2: Raw segments at intersections and ramps:
  - Starting: Raw segments in the immediate downstream of an intersection or a ramp.
  - Ending: Raw segments in the immediate upstream of an intersection or a ramp.

Based on the above criteria, we extract $I^{raw,S}$ and $I^{raw,E}$, which represent sets of S and E-type segments, respectively, from I^{raw}. Segments assigned to both S and E types are removed from $I^{raw,S}$ and $I^{raw,E}$, thereby creating $I^{raw,ISO}$, the set of ISO segments. In other words, for the segments that can be categorized as either starting or ending segments, we isolate them in a separate set $I^{raw,ISO}$.

Next, we merge the raw segments, starting from the first element in $I^{raw,S}$ and following the direction of traffic, to form a list of consecutive segments. As we add segments to the list, we accumulate their lengths in l^{cum}. Once l^{cum} reaches the target length l^{tgt} or we encounter an E-type segment, we stop adding segments to the list. At this point, we merge the list of consecutive segments into a final segment and add it to I. If the termination is triggered by reaching the target length, we append the current raw segment to the last position of $I^{raw,S}$ as a new S-type segment. Finally, we remove the first element of $I^{raw,S}$. This process is repeated until $I^{raw,S}$ becomes an empty set. Then we treat the ISO raw segments as individual final segments and add them to I. It is important to note that although the target length for the final segments is 1 mile, their actual lengths may vary if an E-type segment is encountered earlier or if they belong to the ISO-type

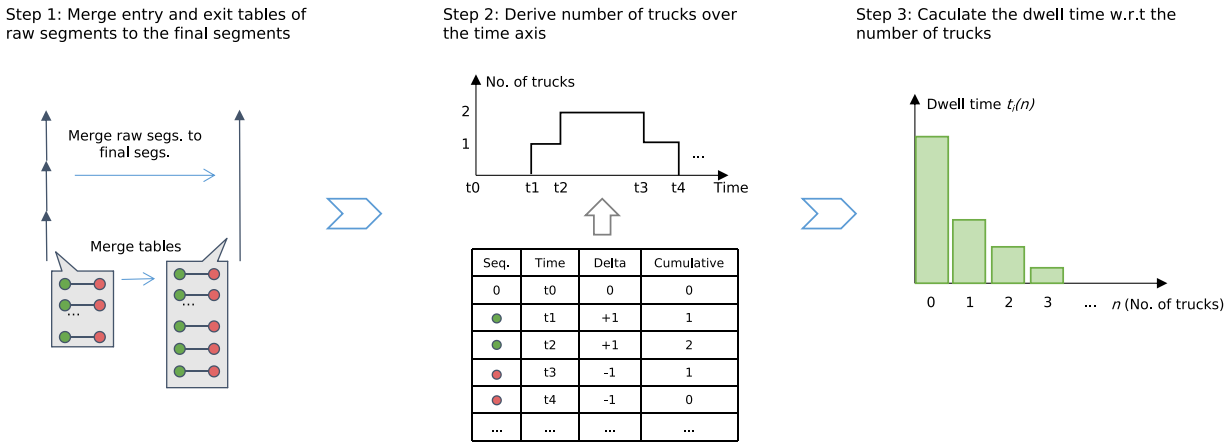

Fig. 17. Procedures to derive dwell time statistics for each final road segment.

segments. However, the majority of final segments still have a length of approximately 1 mile.

Algorithm 2: The algorithm to obtain set I of final road segments

Input : I^{raw}, the set of raw segments. $I^{next}_{i^{raw}}$, the set of adjacent raw segments of raw segment i^{raw} along the direction of traffic.

Output: I, the set of final road segments.

// Find starting/ending/isolated (S/E/ISO) segments.
Identify $I^{raw,S}$, $I^{raw,E}$, and $I^{raw,ISO}$ from I^{raw};

// Merge raw segments.
Initialize empty set $I \leftarrow \emptyset$ to store all final segments;
Initialize target final segment length $l^{tgt} = 1$ mile;
while $I^{raw,S} \neq \emptyset$ **do**
  // Assign current element as the first element in the set $I^{raw,S}$
  Current raw segment $i^{raw} \leftarrow I^{raw,S}(0)$;
  Initialize $list^{current} \leftarrow \{i^{raw}\}$;
  Initialize $l^{cum} = l_{i^{raw}}$;
  while $l^{cum} < l^{tgt}$ & $i^{raw} \notin I^{raw,E}$ **do**
    $i^{raw,next} \leftarrow I^{next}_{i^{raw}}(0)$;
    $list^{current} \leftarrow list^{current} \cup \{i^{raw,next}\}$;
    $l^{cum} \leftarrow l^{cum} + l_{i^{raw,next}}$;
    $i^{raw} \leftarrow i^{raw,next}$;
  end
  if $l^{cum} \geq l^{tgt}$ & $i^{raw} \notin I^{raw,S}$ **then**
    $I^{raw,S} \leftarrow I^{raw,S} \cup i^{raw}$;
  end
  $I^{raw,S} \leftarrow I^{raw,S} \setminus I^{raw,S}(0)$;
  Merge raw segments in $list^{current}$ to a final segment i;
  $I \leftarrow I \cup \{i\}$;
end
$I \leftarrow I \cup I^{raw,ISO}$;
return I

C.2. From GPS data to dwell time statistics

After obtaining I, the set of final segments, our next objective is to gather the dwell time statistics for each segment in I. The overall process is outlined in Fig. 17. Here are the steps involved:

- Step 1: As part of the merging process of raw segments, we also merge the corresponding entry and exit tables of each raw segment with the corresponding final segment.
- Step 2: We sort the entry and exit sequences based on their time points and construct a timetable for each final segment. In this timetable, each entry sequence (green) is linked to an increase of +1 truck, while each exit sequence (red) is linked to a decrease of −1 truck. By tracking the changes in the number of trucks (or the sum of deltas), we can determine the cumulative number of trucks on each segment as a function of time.
- Step 3: In this final step, we derive the truck dwell time on each segment when there are different numbers of trucks on the segment. This results in the calculation of $t_i(n)$ for every segment i in I, where n represents the number of trucks.

By following these steps, we can obtain the dwell time statistics for each segment in I, which are the critical inputs required by the objective function (1).

Appendix D. Estimate congestion costs

In standard highway planning, as outlined in FHWA [59], the assessment of congestion costs necessitates an in-depth, hour-by-hour analysis over a 24-hour period. This involves examining factors like traffic volume, work zone capacity, and potential queuing. For our study, we employed a simplified approach as described in Choi [60], where the daily Road User Cost (RUC) is estimated using the following formula:

$$\text{RUC} = \text{Delay Time} \times \text{Value of Time} \times \text{AADT}$$

In this equation, AADT represents the annual average daily traffic. We have assumed the Delay Time to be attributed solely to reduced speeds. While FHWA [59] provides assumptions regarding work zone speeds and Choi [60] involves empirical measurements of these speeds, our assumptions about work zone speed take into account the varying number of lanes. Specifically, we hypothesize that closure of one lane in a two-, three-, and four-lane highway would reduce the average daily space mean speed by 50%, 40%, and 30%, respectively, and this trend is ongoing for highways with five or more lanes with 10% change for each additional lane until there is no more speed reduction. For the single-lane road segments (mostly ramps), we assume the traffic will be routed onto the road shoulders, making them equivalent to a closure on two-lane ways. The original daily average space mean speed is presumed to be 55 mph and the number of lanes for each segment is estimated based on the peak traffic volumes assuming the capacity is 2,200 vehicles/hour/lane [61]. The Value of Time is set at $25.04 per Choi [60] and has been adjusted to reflect 2023 values considering inflation. For initial estimations, the AADT is presumed to remain constant. The AADT for each road segment i is sourced from the nearest measurement point in Caltrans [62]. Utilizing these parameters,

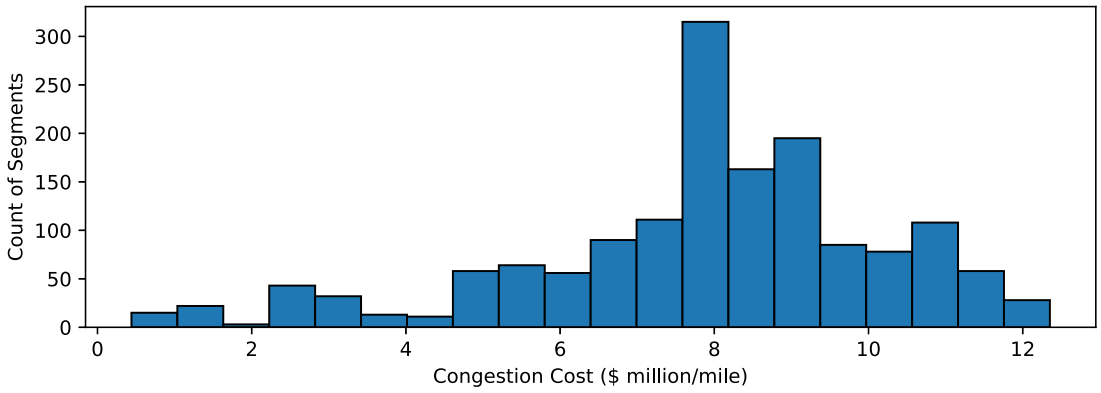

Fig. 18. Histogram of congestion cost.

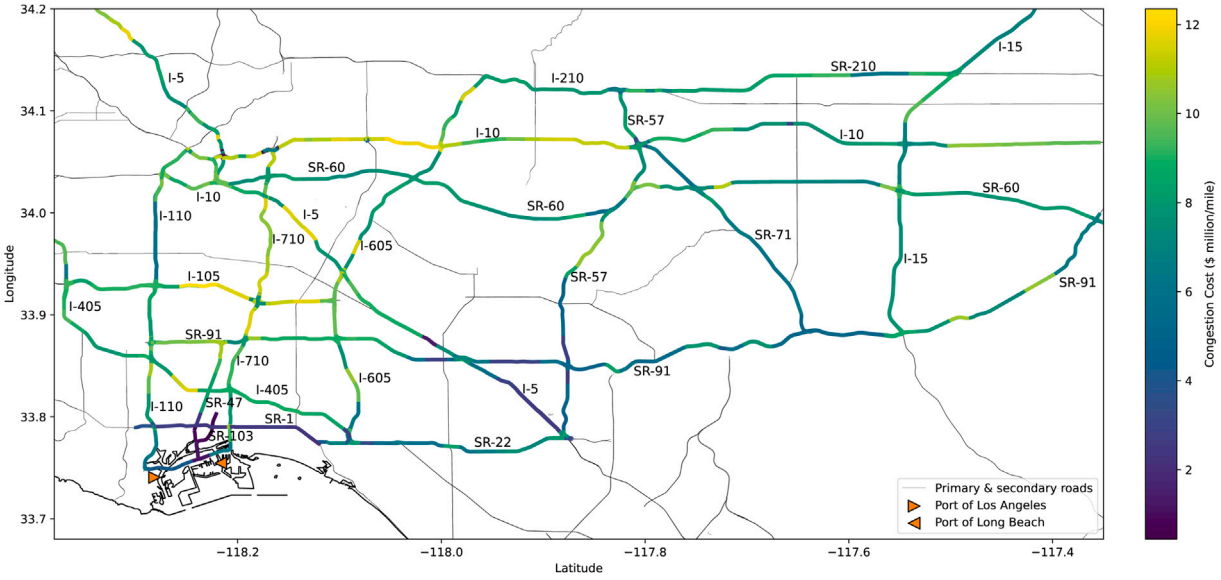

Fig. 19. Geospatial distribution of congestion cost.

we have calculated the congestion cost for each road segment in the set I, assuming the construction would last one year. The distribution of per-mile congestion cost is shown in Fig. 18, ranging between $0.44 million to $12.35 million per mile, with an average of $7.87 million per mile. Fig. 19 further shows the heatmap of congestion costs. In the comparative study presented in Section 7.4, the construction cost will be added to c^{dwcl}, the total cost of DWCLs, and amortized accordingly.

References

[1] USDT. Climate action [online]. 2023, https://www.transportation.gov/priorities/climate-and-sustainability/climate-action. [Accessed May 2023].

[2] Hamidi A, Meroño E. How to decarbonize heavy-duty transport and make it affordable [online]. 2021, https://www.weforum.org/agenda/2021/08/how-to-decarbonize-heavy-duty-transport-affordable/. [Accessed March 2023].

[3] Newsom G. Executive order N-79-20. 2020.

[4] Mulholland E. Europe's new heavy-duty CO_2 standards, explained [online]. 2023, https://theicct.org/eu-co2-hdv-standards-explained-feb23/. [Accessed March 2023].

[5] EPA. Drayage truck best practices to improve air quality [online]. 2023, https://www.epa.gov/ports-initiative/drayage-truck-best-practices-improve-air-quality. [Accessed March 2023].

[6] CARB. CARB fact sheet: 2023 advanced clean fleets regulation - proposed drayage truck requirements [online]. 2023, https://ww2.arb.ca.gov/resources/fact-sheets/carb-fact-sheet-2023-advanced-clean-fleets-regulation-proposed-drayage-truck.

[7] Miller D, Porter M. Electric vehicles are the next dominant class of renewable energy buyers [online]. 2020, https://rmi.org/electric-vehicles-are-the-next-dominant-class-of-renewable-energy-buyers/. [Accessed March 2023].

[8] Tanvir S, Un-Noor F, Boriboonsomsin K, Gao Z. Feasibility of operating a heavy-duty battery electric truck fleet for drayage applications. Transp Res Rec 2021;2675(1):258–68.

[9] Kotz A, Kelly K, Lustbader J, Cary S, Oakleaf B. Port of New York and New Jersey Drayage Electrification Analysis. Technical report, Golden, CO (United States): National Renewable Energy Lab.(NREL); 2022.

[10] Clean Trucks Program. Final 2021 drayage trucks feasibility assessment [online]. 2021, https://cleanairactionplan.org/strategies/trucks/. [Accessed Jan 2024].

[11] Papson A, Ippoliti M. Key performance parameters for drayage trucks operating at the ports of Los Angeles and Long Beach [online]. 2013, https://calstart.org/wp-content/uploads/2018/10/I-710-Project_Key-Performance-Parameters-for-Drayage-Trucks.pdf. [Accessed Jan 2024].

[12] Bradley L. 2019, Charging infrastructure strategies: Maximizing the deployment of electric drayage trucks in Southern California [online].

[13] Afridi K. The future of electric vehicle charging infrastructure. Nat Electron 2022;5(2):62–4.

[14] Mohamed AA, Shaier AA, Metwally H, Selem SI. An overview of dynamic inductive charging for electric vehicles. Energies 2022;15(15):5613.

[15] Taljegard M, Göransson L, Odenberger M, Johnsson F. Spacial and dynamic energy demand of the E39 highway–Implications on electrification options. Appl Energy 2017;195:681–92.

[16] Shi J, Gao HO. Efficient energy management of wireless charging roads with energy storage for coupled transportation–power systems. Appl Energy 2022;323:119619.

[17] Buchholz K. Wireless road charging for EVs to debut in 2023 [online]. 2022, https://www.sae.org/news/2022/06/wireless-road-charging-for-evs. [Accessed Jul 2022].
[18] Askey KA. ORNL demonstrates 120-kilowatt wireless charging for vehicles [online]. 2018, https://www.ornl.gov/news/ornl-demonstrates-120-kilowatt-wireless-charging-vehicles. [Accessed Jul 2022].
[19] Chen Z, Yin Y, Song Z. A cost-competitiveness analysis of charging infrastructure for electric bus operations. Transp Res C 2018;93:351–66.
[20] Konstantinou T, Haddad D, Prasad A, Wright E, Gkritza K, Aliprantis D, et al. Feasibility Study and Design of In-Road Electric Vehicle Charging Technologies. Technical report, Purdue University. Joint Transportation Research Program; 2021.
[21] Limb BJ, Bradley TH, Crabb B, Zane R, McGinty C, Quinn JC. Economic and environmental feasibility, architecture optimization, and grid impact of dynamic charging of electric vehicles using wireless power transfer. 2016.
[22] Majhi RC, Ranjitkar P, Sheng M. Assessment of dynamic wireless charging based electric road system: A case study of Auckland motorway. Sustainable Cities Soc 2022;84:104039.
[23] Brooks KJ. A road in Detroit will charge an electric car while driving [online]. 2022, https://www.cbsnews.com/news/electreon-detroit-wireless-electric-vehicle-charging/. [Accessed Jul 2022].
[24] Carbonaro G. Wireless charging for electric cars is already here - but the technology isn't for everybody yet [online]. 2022, https://www.euronews.com/next/2022/06/24/wireless-charging-roads-for-electric-cars-ev-technology-is-here-fiat-stellantis. [Accessed Jan 2024].
[25] Min R. Sweden is building the world's first permanent electrified road for EVs to charge while driving [online]. 2023, https://www.euronews.com/next/2023/05/09/sweden-is-building-the-worlds-first-permanent-electrified-road-for-evs-to-charge-while-dri. [Accessed Jan 2024].
[26] Ramirez-Ibarra M, Saphores J-DM. Health and equity impacts from electrifying drayage trucks. Trans Res Part D: Trans Environ 2023;116:103616.
[27] Jeong S, Jang YJ, Kum D. Economic analysis of the dynamic charging electric vehicle. IEEE Trans Power Electron 2015;30(11):6368–77.
[28] Liu Z, Song Z. Robust planning of dynamic wireless charging infrastructure for battery electric buses. Transp Res C 2017;83:77–103.
[29] Alwesabi Y, Avishan F, Yanıkoğlu İ, Liu Z, Wang Y. Robust strategic planning of dynamic wireless charging infrastructure for electric buses. Appl Energy 2022;307:118243.
[30] Helber S, Broihan J, Jang YJ, Hecker P, Feuerle T. Location planning for dynamic wireless charging systems for electric airport passenger buses. Energies 2018;11(2):258.
[31] Riemann R, Wang DZ, Busch F. Optimal location of wireless charging facilities for electric vehicles: flow-capturing location model with stochastic user equilibrium. Transp Res C 2015;58:1–12.
[32] Chen Z, Liu W, Yin Y. Deployment of stationary and dynamic charging infrastructure for electric vehicles along traffic corridors. Transp Res C 2017;77:185–206.
[33] Bi Z, Keoleian GA, Lin Z, Moore MR, Chen K, Song L, et al. Life cycle assessment and tempo-spatial optimization of deploying dynamic wireless charging technology for electric cars. Transp Res C 2019;100:53–67.
[34] Li M, Wu X, Zhang Z, Yu G, Wang Y, Ma W. A wireless charging facilities deployment problem considering optimal traffic delay and energy consumption on signalized arterial. IEEE Trans Intell Transp Syst 2019;20(12):4427–38.
[35] Xia F, Chen H, Shahidehpour M, Gan W, Yan M, Chen L. Distributed expansion planning of electric vehicle dynamic wireless charging system in coupled power-traffic networks. IEEE Trans Smart Grid 2021;12(4):3326–38.
[36] He J, Yang H, Tang T-Q, Huang H-J. Optimal deployment of wireless charging lanes considering their adverse effect on road capacity. Transp Res C 2020;111:171–84.
[37] Ngo H, Kumar A, Mishra S. Optimal positioning of dynamic wireless charging infrastructure in a road network for battery electric vehicles. Trans Res Part D: Trans Environ 2020;85:102385.
[38] Liu H, Zou Y, Chen Y, Long J. Optimal locations and electricity prices for dynamic wireless charging links of electric vehicles for sustainable transportation. Transp Res Part E: Logist Transp Rev 2021;152:102187.
[39] Tran CQ, Keyvan-Ekbatani M, Ngoduy D, Watling D. Dynamic wireless charging lanes location model in urban networks considering route choices. Transp Res C 2022;139:103652.
[40] Ushijima-Mwesigwa H, Khan MZ, Chowdhury MA, Safro I. Optimal placement of wireless charging lanes in road networks. J Ind Manag Optim 2021;17(3):1315.
[41] Feng H, Tavakoli R, Onar OC, Pantic Z. Advances in high-power wireless charging systems: Overview and design considerations. IEEE Trans Transp Electr 2020;6(3):886–919.
[42] Bi Z, Kan T, Mi CC, Zhang Y, Zhao Z, Keoleian GA. A review of wireless power transfer for electric vehicles: Prospects to enhance sustainable mobility. Appl Energy 2016;179:413–25.
[43] Southern California Edison. DRPEP terminology [online]. 2023, https://drpep.sce.com/drpep/drpep-interactive-user-guide/#/lessons/TvUrPIf4n1PWtrjeXcXIzvAS0XlxaPwu. [Accessed March 2023].
[44] Alotaibi MA, Salama MM. An incentive-based multistage expansion planning model for smart distribution systems. IEEE Trans Power Syst 2018;33(5):5469–85.
[45] Seta FdS, de Oliveira LW, de Oliveira EJ. Comprehensive approach for distribution system planning with uncertainties. IET Gener Transm Distrib 2019;13(24):5467–77.
[46] Jalali M, Zare K, Hagh MT. A multi-stage MINLP-based model for sub-transmission system expansion planning considering the placement of DG units. Int J Electr Power Energy Syst 2014;63:8–16.
[47] Behzadi S, Bagheri A. A convex micro-grid-based optimization model for planning of resilient and sustainable distribution systems considering feeders routing and siting/sizing of substations and DG units. Sustainable Cities Soc 2023;97:104787.
[48] John J. How transmission along railroads and highways could break open clean energy growth [online]. 2021, https://www.canarymedia.com/articles/transmission/how-transmission-along-railroads-and-highways-could-break-open-clean-energy-growth.
[49] Esri. Make Route Layer (Network Analyst) [online]. 2022, https://pro.arcgis.com/en/pro-app/latest/tool-reference/network-analyst/make-route-layer.htm. [Accessed Apr 2022].
[50] Southern California Edison. Southern california edison DRPEP [online]. 2023, https://drpep.sce.com/drpep/#. [Accessed March 2023].
[51] Nelder C, Rogers E. Reducing EV charging infrastructure costs. Rocky Mountain Institute; 2019.
[52] MISO. Transmission Cost Estimation Guide [online]. 2022, https://cdn.misoenergy.org/20220208PSCItem05cTransmissionCostEstimationGuideforMTEP22_Draft622733.pdf. [Accessed March 2023].
[53] Newnan DG, Eschenbach TG, Lavelle JP. Engineering economic analysis, vol. 1, Oxford University Press; 2004.
[54] Fripp G. What discount rate should be used? [online]. 2024, https://www.clv-calculator.com/discount-rates/discount-rate-used/. [Accessed Jan 2024].
[55] Marcucci T, Tedrake R. Warm start of mixed-integer programs for model predictive control of hybrid systems. IEEE Trans Autom Control 2020;66(6):2433–48.
[56] Miltenberger M. How do I use MIP starts? [online]. 2023, https://support.gurobi.com/hc/en-us/articles/360043834831-How-do-I-use-MIP-starts-. [Accessed March 2023].
[57] Trinko D, Horesh N, Zane R, Song Z, Kamineni A, Konstantinou T, et al. Economic feasibility of in-motion wireless power transfer in a high-density traffic corridor. ETransportation 2022;11:100154.
[58] Esri. ArcGIS API for Python [online]. 2022, https://developers.arcgis.com/python/. [Accessed Mar 2022].
[59] FHWA. Work zone road user costs - concepts and applications [online]. 2011, https://ops.fhwa.dot.gov/wz/resources/publications/fhwahop12005/fhwahop12005.pdf. [Accessed Jan 2024].
[60] Choi J. Road user costs for highway construction projects involving a lane closure. Sustainability 2020;12(8):3084.
[61] FHWA. Simplified highway capacity calculation method for the highway performance monitoring system [online]. 2017, https://www.fhwa.dot.gov/policyinformation/pubs/pl18003/hpms_cap.pdf. [Accessed Jan 2024].
[62] Caltrans. Traffic volumes AADT [online]. 2023, https://gis.data.ca.gov/datasets/d8833219913c44358f2a9a71bda57f76_0. [Accessed Jan 2024].